NATIONAL AERONAUTICS AND SPACE ADMINISTRATION

Technical Report 32-1563

Solar Cell Contact Pull Strength as a Function of Pull-Test Temperature

Robert K. Yasui
Paul A. Berman

JET PROPULSION LABORATORY
CALIFORNIA INSTITUTE OF TECHNOLOGY
PASADENA, CALIFORNIA

August 15, 1972

NATIONAL AERONAUTICS AND SPACE ADMINISTRATION

Technical Report 32-1563

Solar Cell Contact Pull Strength as a Function of Pull-Test Temperature

Robert K. Yasui
Paul A. Berman

JET PROPULSION LABORATORY
CALIFORNIA INSTITUTE OF TECHNOLOGY
PASADENA, CALIFORNIA

August 15, 1972

Preface

The work described in this report was performed by the Guidance and Control Division of the Jet Propulsion Laboratory.

Page Intentionally Left Blank

Contents

Tables

Figures

Contents (contd)

Figures (contd)

Contents (contd)

Figures (contd)

Abstract

Four types of solar cell contacts were given pull-strength tests at temperatures between −173 and +165°C. Contacts tested were (1) solder-coated titanium–silver contacts on *n–p* cells, (2) palladium-containing titanium–silver contacts on *n–p* cells, (3) titanium–silver contacts on 0.2-mm-thick *n–p* cells, and (4) solder-coated electroless-nickel-plated contacts on *p–n* cells. Maximum pull strength was demonstrated at temperatures significantly below the air mass zero cell equilibrium temperature of +60°C. At the lowest temperatures, the chief failure mechanism was silicon fracture along crystallographic planes; at the highest temperatures, it was loss of solder strength. In the intermediate temperatures, many failure mechanisms operated. Pull-strength tests give a good indication of the suitability of solar cell contact systems for space use, and the tests reported here were the first to be carried out under simulated spaceflight temperatures. Procedures used to maximize the validity of the results are described in detail.

Solar Cell Contact Pull Strength as a Function of Pull-Test Temperature

I. Introduction

Contact pull-strength tests are one of the most important tools for evaluating the suitability of solar cell contact systems for space use; there is no known alternative that can provide similar information. Such testing can not only give information about the mechanical integrity of the contact, but can also be used to isolate the various failure modes and provide information for improving cell design.

There are two major sources of solar cell degradation. One source involves degradation of solar cell electrical characteristics as a result of exposure to radiation; the second source is a degradation of electrical and/or mechanical solar cell characteristics as a result of contact deterioration due to exposure to storage and space ambient conditions. The authors have presented the results of extensive investigations of the second source of cell degradation, contact deterioration, in previous Jet Propulsion Laboratory (JPL) technical reports (Refs. 1 and 2). These reports dealt with exposure of the cells to various temperatures, with and without the addition of a high-humidity ambient, and compared exposed and unexposed cell electrical and mechanical characteristics.

All results in these earlier studies were normalized to the temperature at which the measurements were made (ordinarily, room temperature). This is not, of course, the usual condition under which cells actually operate; when the contacts are in use, the stresses imposed on them occur at spaceflight temperatures, not at room temperature—a fact that is especially important for the study of mechanical characteristics. Consequently, to further improve the knowledge of cell contact mechanical characteristics, the pull-strength tests described in the present report were performed at temperatures that ranged between $-173°C$ and $+165°C$. A surprising result was that most contact systems that were tested exhibited their maximum contact strength at a temperature below 0°C, with rather rapid decreases in contact strength observed at temperatures above and below the maximum-strength temperature.

A second objective of this report is to define more extensively the actual techniques used in the performance of the contact pull-strength test. It has become increasingly apparent to the authors, after discussions with recipients of the previous JPL technical reports (Refs. 1 and 2), that standardization of the contact pull-testing techniques is necessary throughout the industry. Even the very best cells can be made to fail at relatively low contact pull-stresses if improper testing procedures are used. This is particularly disturbing since, at the present time, there is no substitute for contact pull-strength

tests. The authors have clearly shown (Refs. 1–3) that the results of electrical testing cannot be used to infer the mechanical condition of the contacts. Furthermore, the contact pull tests not only determine the strength of the contact, but by proper interpretation of the condition of the cell and the test tab after separation, the exact nature of the weakness can also be determined (e.g., poor plating or evaporation, silicon stress, poor soldering, etc.).

On the subject of contact failure modes, the authors would like to explode a myth prevalent in the industry that a "good" contact is one in which the silicon pulls out, leaving the contact relatively intact. This is not necessarily the case, since excessive solder build-up on the contact of a cell that has undergone temperature cycling (especially to low temperatures) will result in severe stresses in the silicon due to the thermal coefficient mismatch among the silicon, the bus bar, and the solder, and these stresses will cause the silicon to fracture at very low pull strength values. Similarly, cell breakage under low applied load conditions can indicate internal stresses, microcracks, crystalline defects, or other mechanical defects due to poor processing. Such defects can result from inadequate control of metal evaporation, solder alloy, crystal growth, slabbing, slicing, and/or lapping.

A third objective of this study is to provide data to be used as input to a stress analysis computer program which has been on-going at JPL for the past several years (Refs. 4 and 5) and to determine the validity of the modeling. The goals of this computer program are (1) prediction of the stresses induced in any cell contact–interconnection system as a result of exposure to any environment or series of environments, (2) determination of the environmental extremes to which a given cell contact–interconnection can be exposed without inducing failure of any part of the system and (3) optimization of the cell contact–interconnection system as a function of environmental exposure.

II. Contact Pull-Strength Test Materials, Facility, and Procedure

The configurations and specifications associated with the contact test tabs are shown in Fig. 1. As noted in this figure, the tabs are fabricated from tin-plated, photo-etched Kovar (iron, nickel, and cobalt alloy), having a thickness of 0.1 mm. Each test tab is bent in a forming fixture at a 90-deg angle before being soldered to the cell. The soldering operation is accomplished semiautomatically by use of a Sippican RS-333 Reflow Soldering System.[1] A solder preform is added to all non-solder-coated solar cells, normally having a composition of 62% tin, 36% lead, and 2% silver. When non-solder-coated cells were to be tested at temperatures above 190°C, however, the preform was fabricated from Alpha solder No. 32, which has a higher tin-to-lead ratio and exhibits a higher melting point than the 62–36–2 Sn–Pb–Ag solder preform (which becomes plastic at approximately 165°C). For the solder-coated cells, no preform was used.

The area on the cell contact to which the tabs may be soldered is carefully defined, as shown in Fig. 2, to eliminate extraneous effects and to enhance the uniformity of cell-to-cell contacts. After soldering, the tab is inspected to ensure its location within the area allowed, as shown in Fig. 2, and to determine that the joint itself is acceptable according to the criteria shown in Fig. 3. The solder joint area, assuming an additional area of about 10% for the solder fillet, was calculated to be 3.42 mm^2. Tab-cell joints that exhibit excessive solder, incomplete solder, or an incomplete solder joint are rejected and not tested. It has been found that many apparent inconsistencies in contact pull-strength results are the result of improper tab soldering techniques and that strict adherence to the solder joint inspection criteria defined in Figs. 2 and 3 are mandatory if meaningful results are to be obtained.

To minimize electrode heating during the soldering reflow operation, the solder time–temperature profile or heat cycle is pulsed twice at a reduced voltage to obtain consistent and uniform soldering. An applied electrode load of 3.3 kg is used, and a total elapsed time of about 4 s for each soldering operation is maintained. This operator-independent soldering technique was developed to minimize the effects of variations in the soldering operation. A second major source of anomalous pull-strength test results has been found to result from variations in the soldering technique, and the precise control associated with the technique described has served to greatly minimize such variations.

The contact pull-strength tests are performed with an Instron Universal Material Test Machine[2] Model TM-1 and a self-contained portable temperature-controlled chamber. A special test fixture is used, which adapts to cells of varying dimensions so that they can be mounted and properly aligned perpendicular to the direction of the applied load. A copper–constantan thermocouple is mounted between the test specimen and the test fixture

[1]Sippican Corp., Industrial Products Division, Mattapoisett, Mass.
[2]Instron Engineering Corp., Long Beach, Calif.

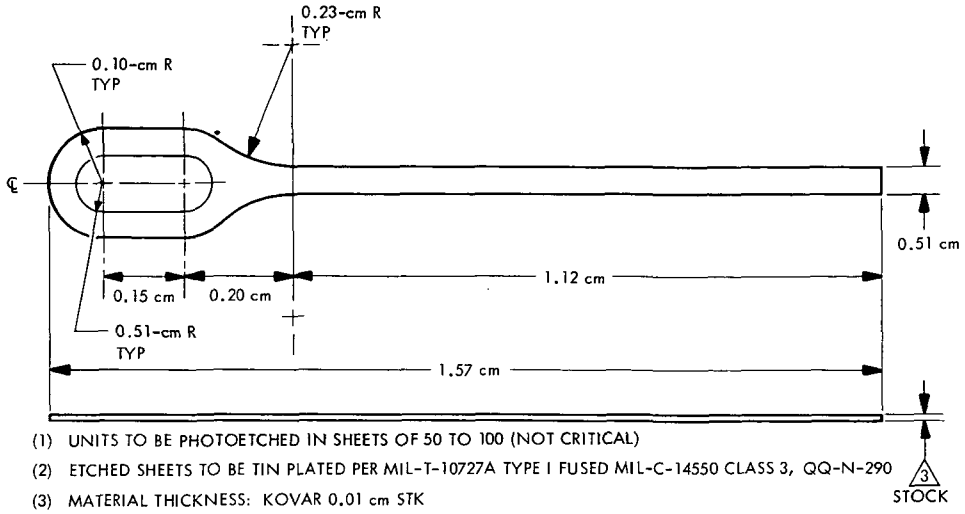

Fig. 1. Solar cell ohmic contact strength test tab

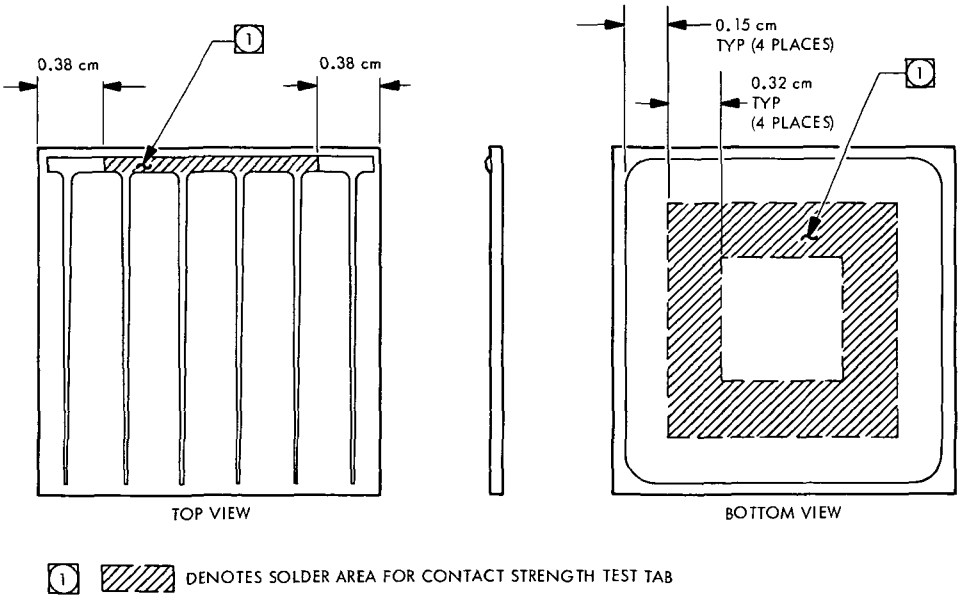

Fig. 2. Definition of area for pull-test tab soldering

so that cell temperature can be monitored and maintained at the desired value. The contacts are pulled at a constant rate of 0.084 ±0.008 cm/s, which corresponds to 5.04 cm/min, until complete separation occurs. A third major source of anomalous pull strength test results has been found to be associated with variations in the pull rate, and careful control of the pull rate minimizes variations in pull strength. The resultant contact strength is recorded on a strip chart recorder in the form of a stress–strain characteristic curve. After separation, the test specimens are reinspected and analyzed for the interfacial characteristics that led to the separation (e.g., solder failure, contact delamination, broken cells, defective tabs, etc.). A schematic showing the contact strength test configuration is given in Fig. 4. By careful control of the materials, processes, techniques, and inspections involved in performing the contact pull-strength tests, the effects of extraneous variables on the test results were minimized and the validity of the test results greatly enhanced.

III. Results

Altogether, 690 contacts were tested, and 16 different temperatures were included in the test program. The cells were manufactured either by Centralab[3] or Heliotek[4] and were of four different types: (1) solder-coated titanium–silver contacts on *n–p* cells, (2) palladium-containing titanium–silver contacts on *n–p* cells, (3) titanium–silver contacts on 0.2-mm-thick *n–p* cells, and (4) solder-coated electroless-nickel-plated contacts on *p–n* cells. Testing temperatures and results for the four types of contacts are presented in the following sections.

A. Solder-Coated Titanium–Silver Contacts on *n–p* Cells

The description of the cell type and the number of cells tested at each temperature are presented in Table 1. As noted, this cell type has been used on the *Mariner* 1969 and *Mariner* 1971 flight spacecraft. A total of 115 cells were evaluated, representing testing of 230 contacts, since both *p* and *n* contacts were tested. The cells were tested over a temperature range of −173.3 to +165.5°C.

The contact strengths of the *n*, or diffused layer, contacts as functions of temperature are summarized in Fig. 5, which shows the average contact strength, the 95% confidence limits, and a least squares fit to the data. It can be seen from this figure that the maximum contact strength is obtained at a temperature of approximately −73°C. At this temperature, the least squares fit indicates that the contact strength is about 2500 g. The 95% confidence limits indicate larger spreads at temperatures between −73 and −145°C. This trend appears to be reversed at the lowest temperature of −173°C, where the confidence limits are of the same order as those of temperatures between −29 and +82°C. At temperatures of 110°C and above, the confidence limits become quite small because the plasticity of the solder is the dominant effect, whereas at the lower temperatures many more failure mechanisms are operating and competing.

Table 1. Test conditions, solder-coated titanium–silver contacts on *n–p* cells[a]

Number of cells tested[b]	Test temperature	
	°C	°F
10	−173.3	−280
10	−145.6	−230
10	−112.2	−170
10	−84.4	−120
10	−56.7	−70
10	−28.9	−20
10	−1.1	30
10	26.7	80
10	54.4	130
10	82.2	180
5	110.0	230
5	137.8	280
5	165.5	330
0	190.5	375
0	204.4	400
0	218.0	425

[a]Base resistivity = 2 Ω-cm
Nominal dimensions
Size = 2 × 2 cm
Thickness = 0.046 cm (18 mils)
Vendor—Heliotek.
Flight history—*Mariner* 1969 and *Mariner* 1971.
[b]Total number of contacts evaluated ($p + n$) = 230.

The data are presented in a similar manner for the strength of the *p*, or base region contact, as a function of temperature (Fig. 6). It can be seen that the results of the *p* contact strength tests are very similar to the results of the *n* contact strength tests, the maximum contact strength also being achieved at a temperature of approximately −73°C. In this case, the confidence limits appear to be more consistent and slightly larger than for the *n* contacts, but at the highest and lowest temperatures they are similar to the *n* contact results.

[3]Centralab, The Electronics Division of Globe-Union, Inc., Milwaukee, Wis.

[4]Heliotek, a Division of Textron Inc., Sylmar, Calif.

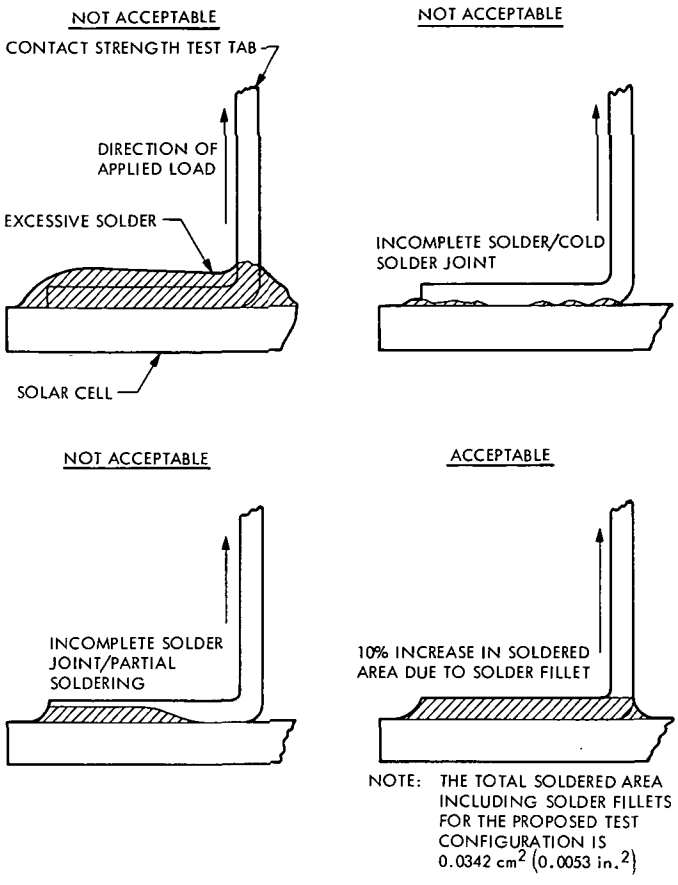

Fig. 3. Solder joint acceptance/rejection criteria

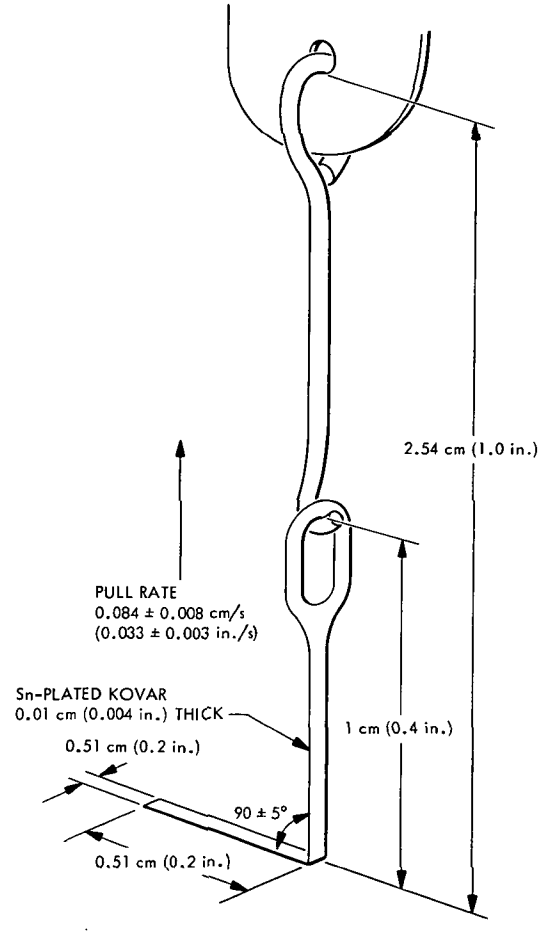

Fig. 4. Contact strength test configuration

Inspection of the p contacts and tabs after separation of the contact test tabs indicated that for the lowest temperature of -173.3°C, the dominant failure mode was pulled silicon. A typical result of a pull-to-failure test at temperatures between -112 and -173°C is shown in Fig. 7. The separated tab shows gross silicon removal, the silicon having a structured appearance typical of stressed silicon. The tab also exhibits separation of the contact metal from the silicon surface. At temperatures between -57 and -29°C, the major failure mechanism was actual breakage of the contact tab, as shown in Fig. 8. This indicates that the contact strength at these temperatures is, in general, greater than the strength of the tab itself, which represents a highly desirable condition. At temperatures between -1 and $+82$°C, the major causes of failure consisted of pulled solder or separation of the metallic contact from the silicon surface, as shown in Fig. 9. At temperatures between $+110$ and 165°C, the failure mechanism is almost exclusively due to pulled solder, as shown in Fig. 10, resulting from the solder's becoming plastic at these elevated temperatures and significantly losing strength.

Similar results were observed in the separated tabs from the p or base region contact shown in Figs. 11–14. The same trend is observed for the p contact failure mechanism modes, namely, fracture of silicon at the low temperatures, breaking of the contact tab at about -70°C, separation of metallic contact from the silicon surface, separation of the solder at intermediate temperatures, and, almost always, separation of the solder at the higher temperatures.

B. Palladium-Containing Titanium–Silver Contacts on *n–p* Cells

The cell description and sample sizes are given in Tables 2 and 3. Cells supplied by both Heliotek and Centralab were investigated. Fifty cells or 100 contacts were evaluated for each manufacturer's cells. Solder preforms were used in all cases to attach the pull test tabs. As discussed previously, cells which were to be measured at temperatures above 190°C made use of a special high-temperature solder preform.

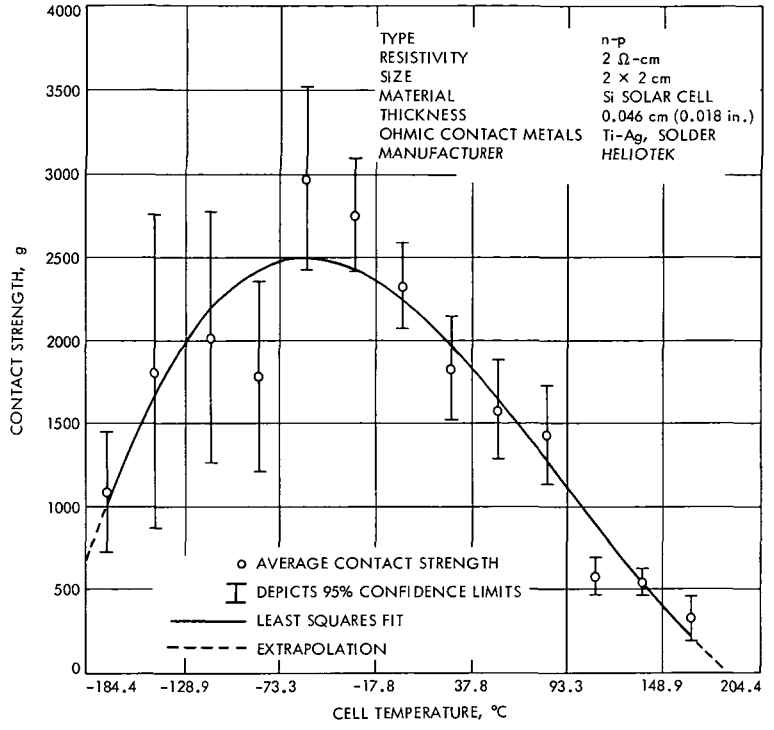

Fig. 5. *n*-contact strength, solder-coated titanium–silver contacts on *n–p* cells, as a function of temperature

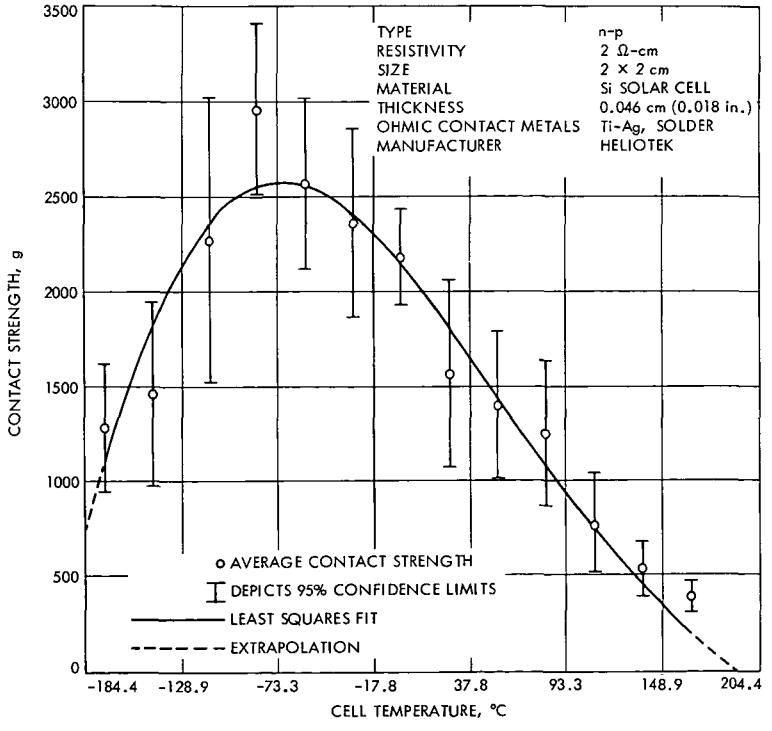

Fig. 6. *p*-contact strength, solder-coated titanium–silver contacts on *n–p* cells, as a function of temperature

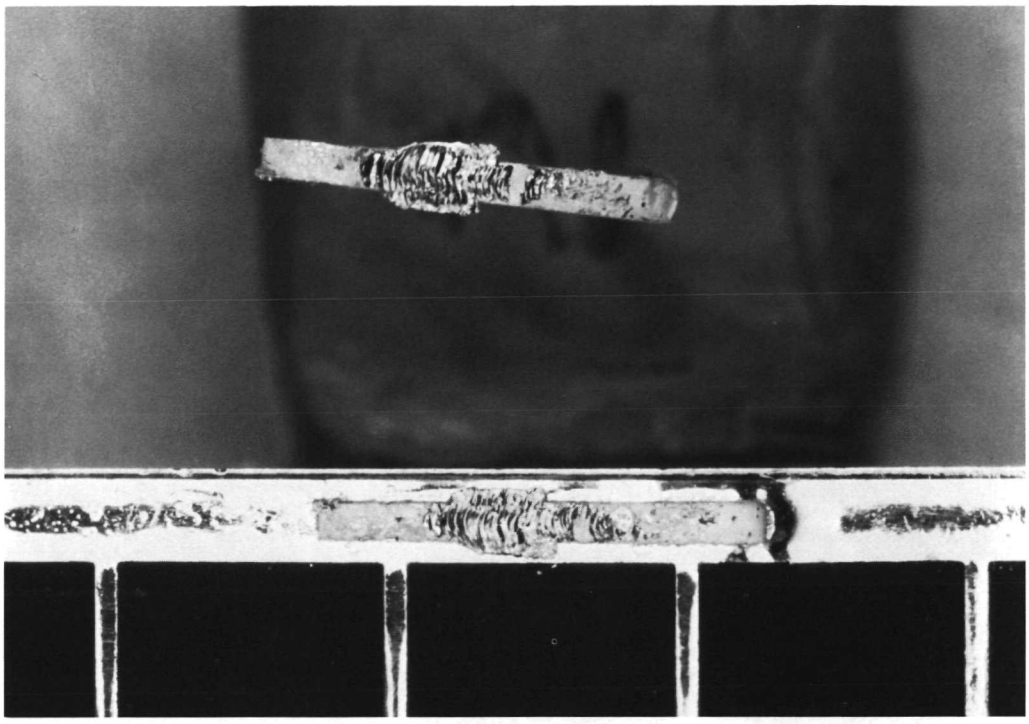

Fig. 7. Typical failure mode of *n* contact, solder-coated titanium–silver contacts on *n–p* cells, over a pull-test temperature range of −112 to −173°C

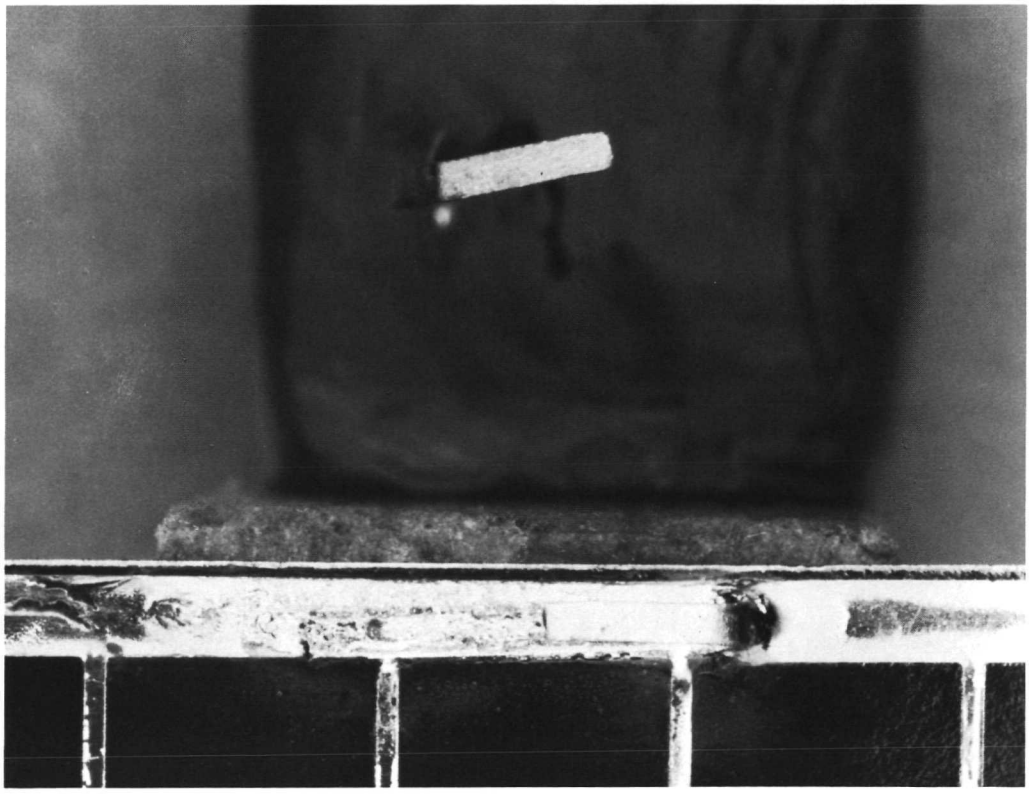

Fig. 8. Typical failure mode of *n* contact, solder-coated titanium–silver contacts on *n–p* cells, over a pull-test temperature range of −29 to −84°C

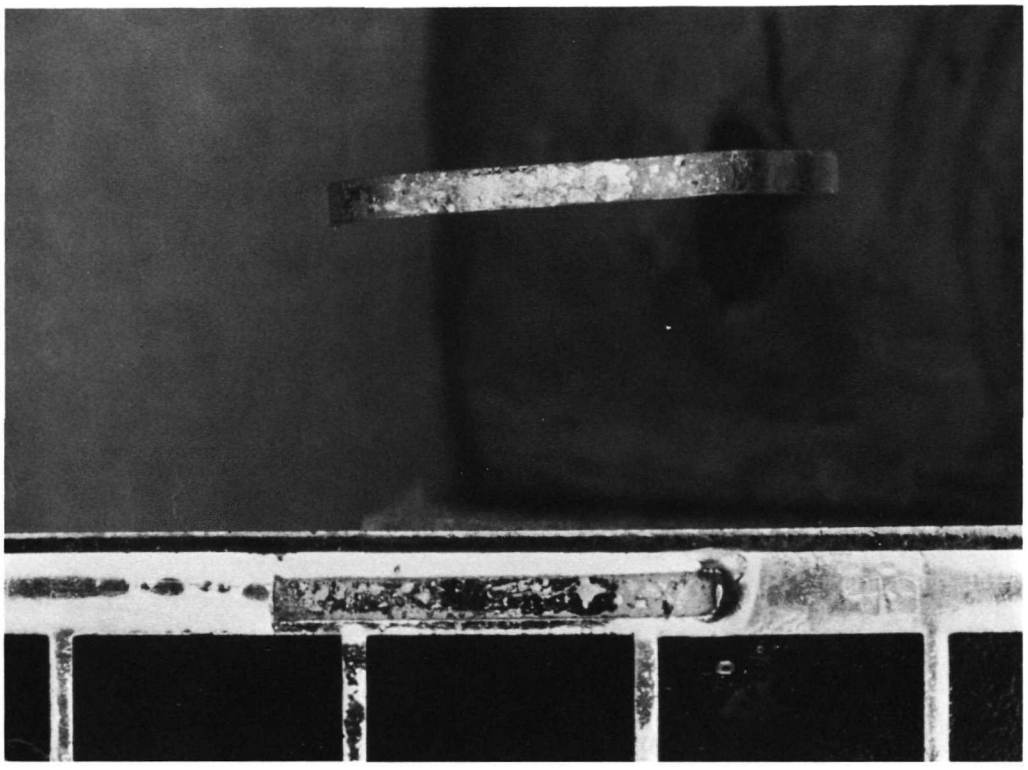

Fig. 9. Typical failure mode of *n* contact, solder-coated titanium–silver contacts on *n–p* cells, over a pull-test temperature range of −1 to +82°C

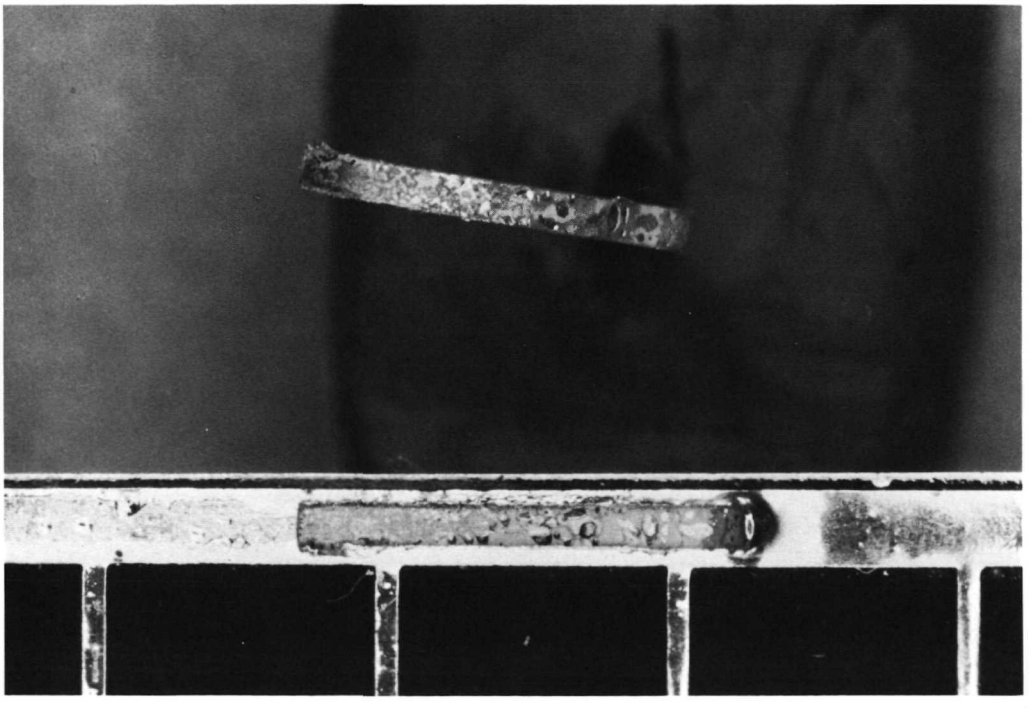

Fig. 10. Typical failure mode of *n* contact, solder-coated titanium–silver contacts on *n–p* cells, over a pull-test temperature range of +110 to +165°C

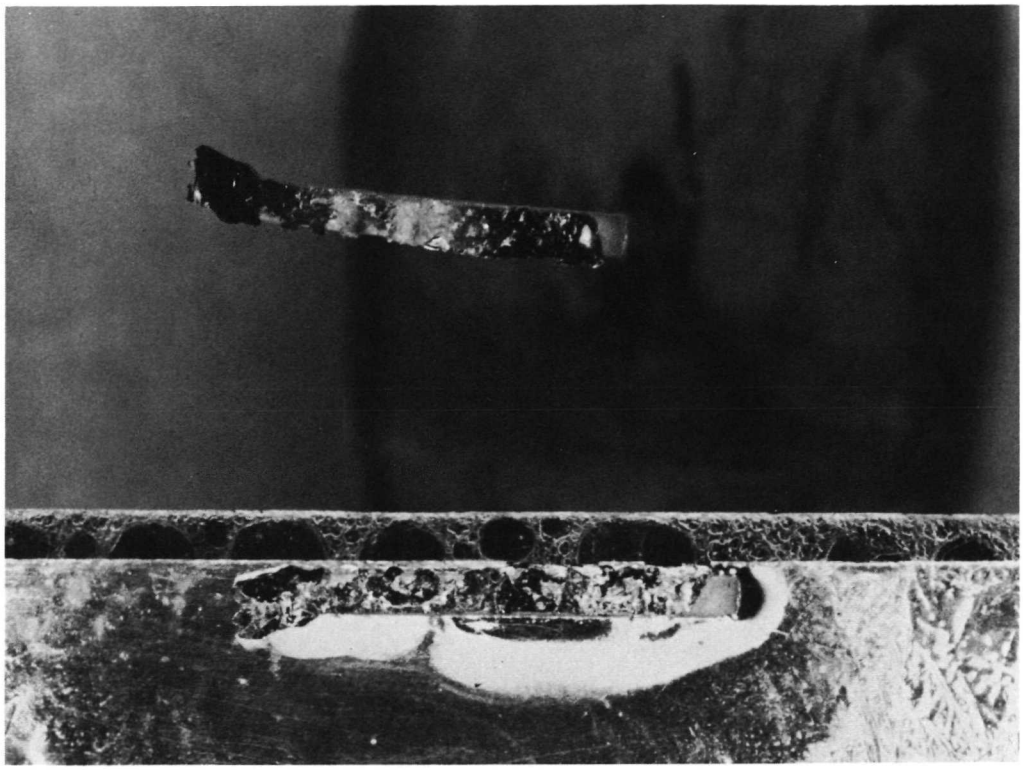

Fig. 11. Typical failure mode of *p* contact, solder-coated titanium–silver contacts on *n–p* cells, over a pull-test temperature range of −112 to −173°C

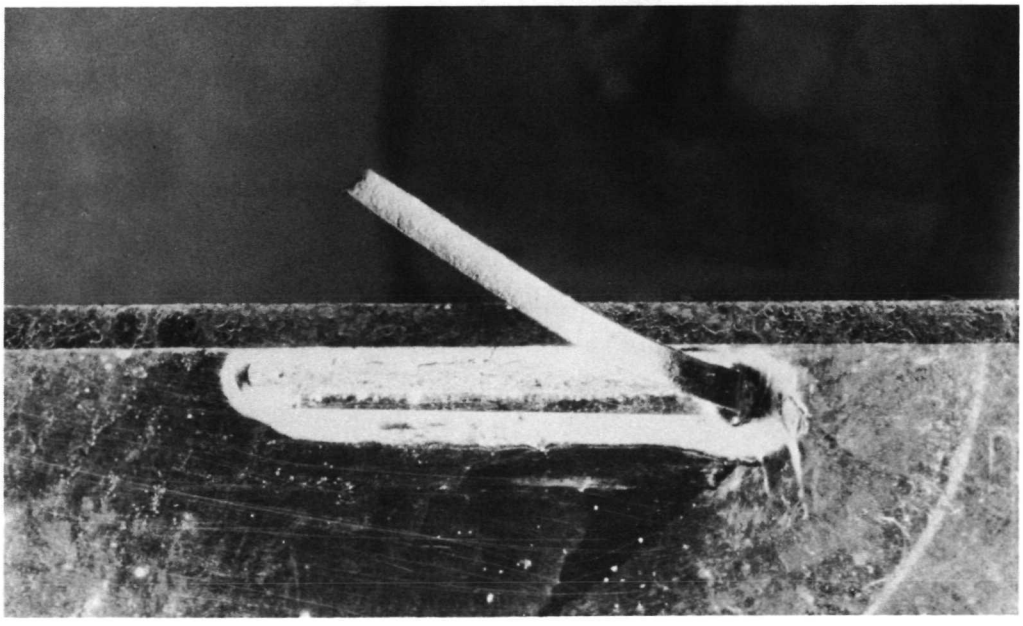

Fig. 12. Typical failure mode of *p* contact, solder-coated titanium–silver contacts on *n–p* cells, over a pull-test temperature range of −29 to −84°C

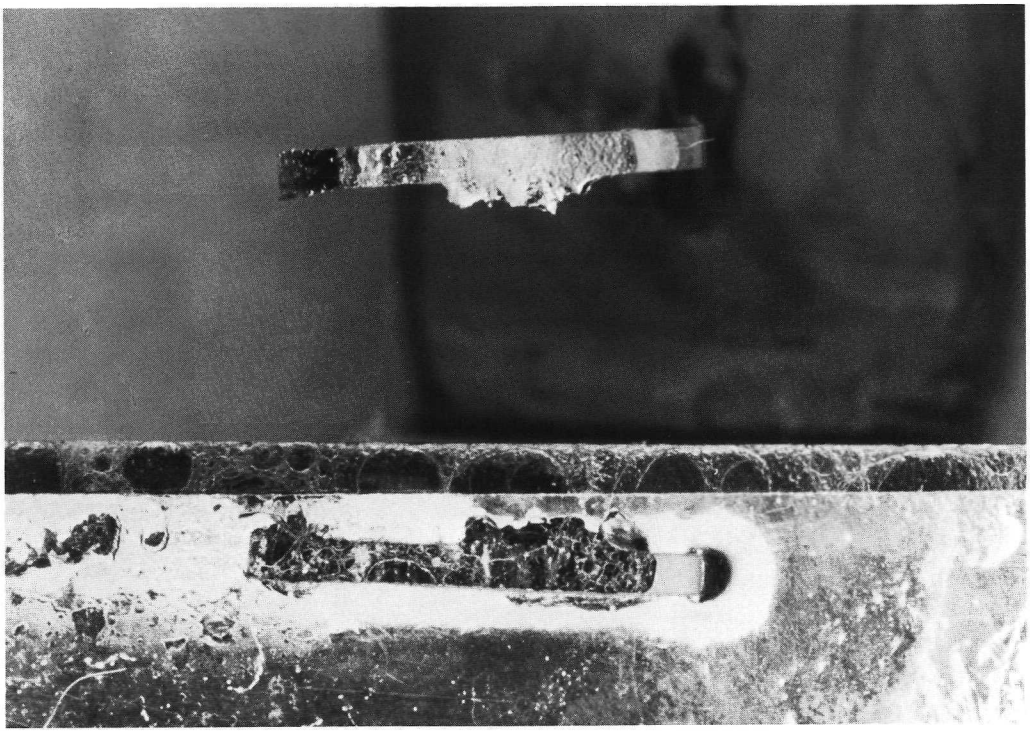

Fig. 13. Typical failure mode of *p* contact, solder-coated titanium–silver contacts on *n–p* cells, over a pull-test temperature range of −1 to +82°C

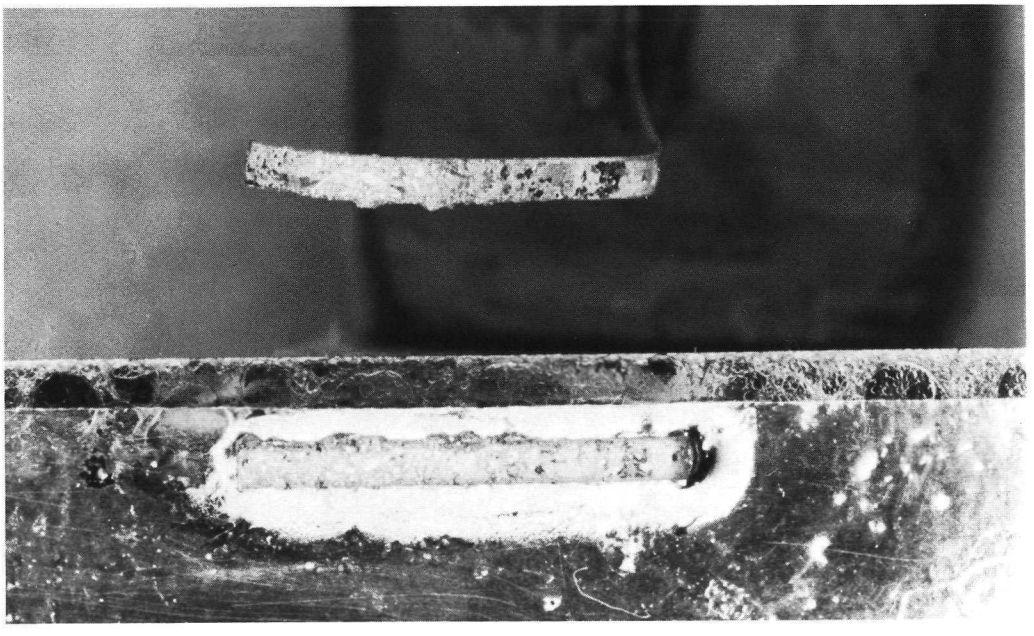

Fig. 14. Typical failure mode of *p* contact, solder-coated titanium–silver contacts on *n–p* cells, over a pull-test temperature range of +110 to +165°C

Table 2. Test conditions, palladium-containing titanium–silver contacts on *n–p* cells (Heliotek)[a]

Number of cells tested[b]	Test temperature	
	°C	°F
5	−173.3	−280
0	−145.6	−230
5	−112.2	−170
0	−84.4	−120
0	−56.7	−70
5	−28.9	−20
0	−1.1	30
5	26.7	80
0	54.4	130
5	82.2	180
0	110.0	230
5	137.8	280
5	165.5	330
5	190.5	375
5	204.4	400
5	218.0	425

[a]Base resistivity = 2 Ω-cm
Nominal dimensions
Size = 2 × 2 cm
Thickness = 0.046 cm (18 mils)
Flight history—none; research and development only.
[b]Total number of contacts evaluated ($p + n$) = 100.

Table 3. Test conditions, palladium-containing titanium–silver contacts on *n–p* cells (Centralab)[a]

Number of cells tested[b]	Test temperature	
	°C	°F
5	−173.3	−280
0	−145.6	−230
5	−112.2	−170
0	−84.4	−120
0	−56.7	−70
5	−28.9	−20
0	−1.1	30
5	26.7	80
0	54.4	130
5	82.2	180
0	110.0	230
5	137.8	280
5	165.5	330
5	190.5	375
5	204.4	400
5	218.0	425

[a]Base resistivity = 2 Ω-cm
Nominal dimensions
Size = 2 × 2 cm
Thickness = 0.046 cm (18 mils)
Flight history—none; research and development only.
[b]Total number of contacts evaluated ($p + n$) = 100.

The pull-strength results on the *n* or diffused-surface contact of the Heliotek cells are shown in Fig. 15 as a function of pull-test temperature. In a manner similar to that of Figs. 5 and 6, the average strength, the 95% confidence limits, and a least squares fit to the data are shown. The overall shape of the curve is somewhat different from that of Fig. 5. Maximum contact strength seems to be achieved at a temperature of about −112°C. The fall-off in contact strength is not as rapid at the higher temperatures, because of the higher melt-temperature solder used to attach the contact tab. The highest contact strength observed for this contact, which is about 1000 g, is considerably lower than that of the solder-coated titanium–silver contact system depicted in Fig. 5. The latter showed a maximum contact strength of 2500 g at a temperature of −73°C, and in fact the contact pull-strength fell below 1000 g only at temperatures in excess of about 90°C, where the solder started to become plastic.

Figure 16 shows similar results for the Heliotek *p* or base-region palladium-containing titanium–silver contact. Here again the absolute pull strengths were significantly below those of comparable cells of Fig. 6 (solder-coated titanium–silver base region contact), and indicate that maximum contact strength occurs at about −112°C. At the lower temperatures, the prevalent failure mode still appeared to be silicon fracture; however, there was a considerable amount of solder failure as well. In fact, failure of the solder was quite prevalent throughout the entire temperature range. At the intermediate temperatures, separation of the metallized contact from the silicon surfaces was also noted.

The contact strength of the Centralab *n* or diffused-sheet contact as a function of pull-test temperature is shown in Fig. 17. This figure, which shows the average contact strength at each of the test temperatures, the 95% confidence limits, and a least squares fit to the data, can be compared with Fig. 15, which depicts the contact strength as a function of pull-test temperature of the diffused-sheet contact of Heliotek cells utilizing the same contact system. The shape of the curve associated with the Centralab cells is somewhat different from that of the curve associated with the Heliotek cells. Whereas the Heliotek cells exhibited a maximum strength at a temperature of about −112°C, the Centralab cells exhibited maximum contact strength at a temperature of about −29°C. The maximum contact strengths, however, are comparable. The contact strength of the Centralab cell at −173°C appears to be considerably lower than that of the Heliotek cells at the same temperature, the former exhibiting a strength below 500 g and the latter a strength above 600 g.

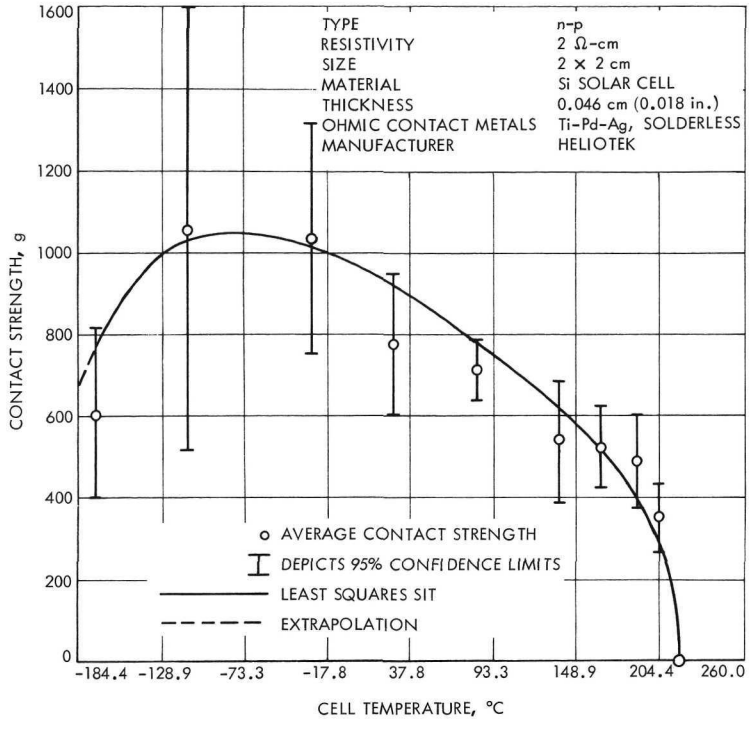

Fig. 15. *n*-contact strength, palladium-containing titanium–silver contacts on *n–p* cells (Heliotek), as a function of temperature

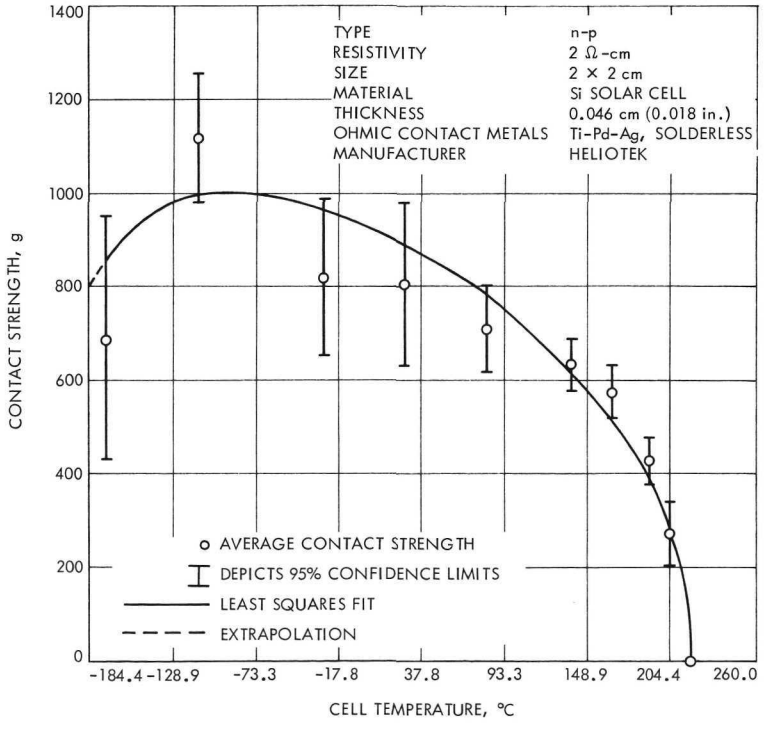

Fig. 16. *p*-contact strength, palladium-containing titanium–silver contacts on *n–p* cells (Heliotek), as a function of temperature

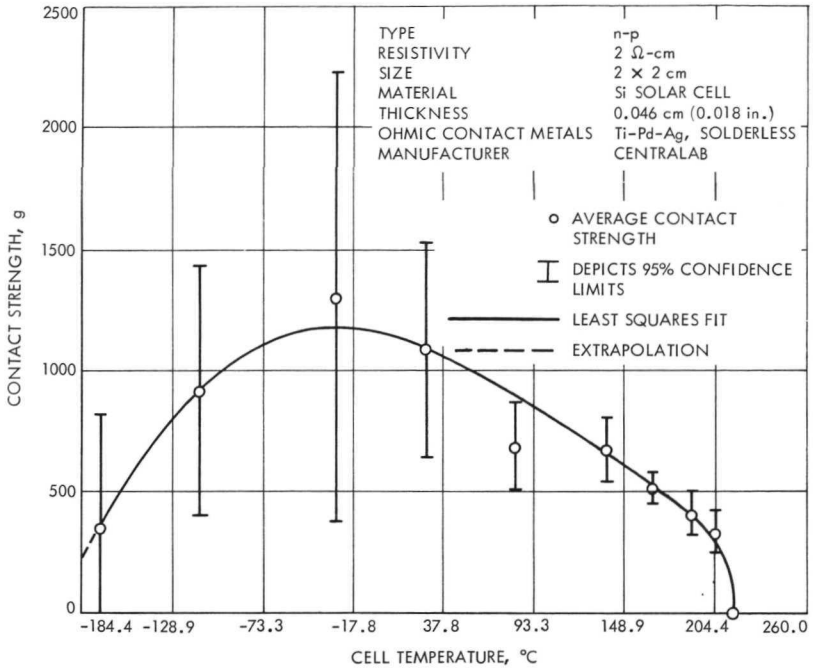

Fig. 17. *n*-contact strength, palladium-containing titanium–silver contacts on *n–p* cells (Centralab), as a function of temperature

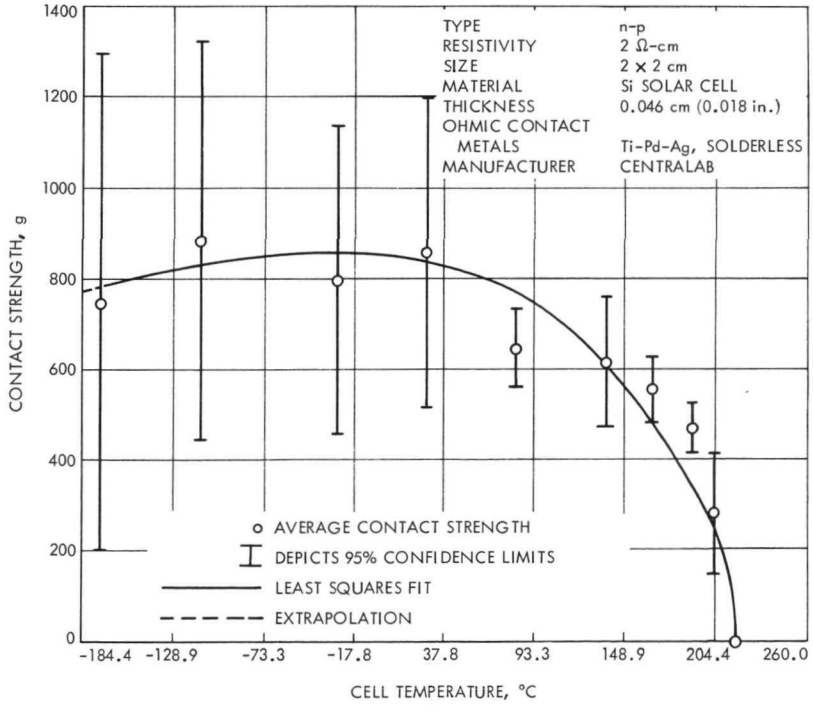

Fig. 18. *p*-contact strength, palladium-containing titanium–silver contacts on *n–p* cells (Centralab), as a function of temperature

The contact strength of the p or base-region contact as a function of cell temperature is shown in Fig. 18 and may be compared with Fig. 16 for the Heliotek cells utilizing the same contact system. Here again, the shape of the curves appears to be somewhat different. The Heliotek cells exhibited a fairly sharp peak in contact strength of 1000 g at a temperature of about −112°C, whereas the curve appropriate to the Centralab cells appeared to be not nearly as peaked. The pull-strength tests of the Centralab p contacts indicated a maximum contact strength of about 850 g at a temperature of −29°C, similar to that observed for the n contact of these cells, as shown in Fig. 18. The p contact strength of the Centralab cells at −173°C (750 g) was significantly higher than that of the n contact strength of the cells at this temperature and is comparable with the contact strengths of the Heliotek cells using the same contact system at −173°C.

It is concluded that the curves associated with the n and p contact pull strength as a function of temperature for the palladium-containing titanium–silver contact system from the same manufacturer are quite similar, but that there is an apparent difference in the mechanical characteristics of the contacts between the manufacturers.

C. Titanium–Silver Contacts on 0.2-mm-Thick *n–p* Cells

The cell description and the number of cells tested at each temperature are shown in Table 4. A sample size of 10 was used over the temperature range of −173 to +82°C and a sample size of 5 was used over the temperature range of 110 to 165°C. Sixty-five cells in all were evaluated, corresponding to testing of 130 contacts. These cell types are representative of those upon which lightweight solar arrays are predicated. Solder preforms were utilized to facilitate attachment of the pull-test tabs.

The results of the contact pull tests on the n or diffused layer contact are shown as a function of cell temperature in Fig. 19. This figure corresponds to Figs. 5, 15, and 17, previously discussed. The overall shape of the least squares fit is more similar to that of Fig. 5 (the solder-coated titanium–silver contact cells) than to that of Figs. 15 and 17 (the palladium-containing titanium–silver cells). Figure 19 indicates that maximum contact strength is achieved at a temperature of about −29°C as opposed to the approximate −73°C maximum contact strength temperature indicated for the previous contact systems discussed. It should be noted, however, that this curve is based on the least squares fit and not on the actual data points. The maximum contact strength was about 1700 g, which is significantly higher than that of the palladium-containing titanium–silver contact system but considerably below that of the solder-coated titanium–silver system. Furthermore, the overall spread in results as indicated by the 95% confidence limits appears to be greater than for the previously discussed contact systems.

Table 4. Test conditions, titanium–silver contacts on 2-mm-thick *n–p* cells[a]

Number of cells tested[b]	Test temperature	
	°C	°F
10	−173.3	−280
10	−145.6	−230
10	−112.2	−170
10	−84.4	−120
10	−56.7	−70
10	−28.9	−20
10	−1.1	30
10	26.7	80
10	54.4	130
10	82.2	180
5	110.0	230
5	137.8	280
5	165.5	330
0	190.5	375
0	204.4	400
0	218.0	425

[a]Base resistivity = 2 Ω-cm

Nominal dimensions
Size = 2 × 2 cm
Thickness = 2 mm (8 mils)

Vendor—Heliotek.

Flight history—research and development, 20 W/lb program and roll-up array for Air Force spacecraft.

[b]Total number of contacts evaluated ($p + n$) = 130.

Similar results are shown for the p or base-region contact pull strength as a function of temperature in Fig. 20. Here again the maximum contact strength is below that of the solder-coated titanium–silver system and above that of the palladium-containing titanium–silver contact system. The spread in results as indicated by the 95% confidence limits is again larger than that for the previous two cell types.

Because the 0.2-mm-thick cells are considerably more fragile than the normal cells, which have three to four times the thickness, the cells were bonded to an aluminum plate having face dimensions of 2 × 2 cm and a thickness of 5.45 mm. The bonding was done by means

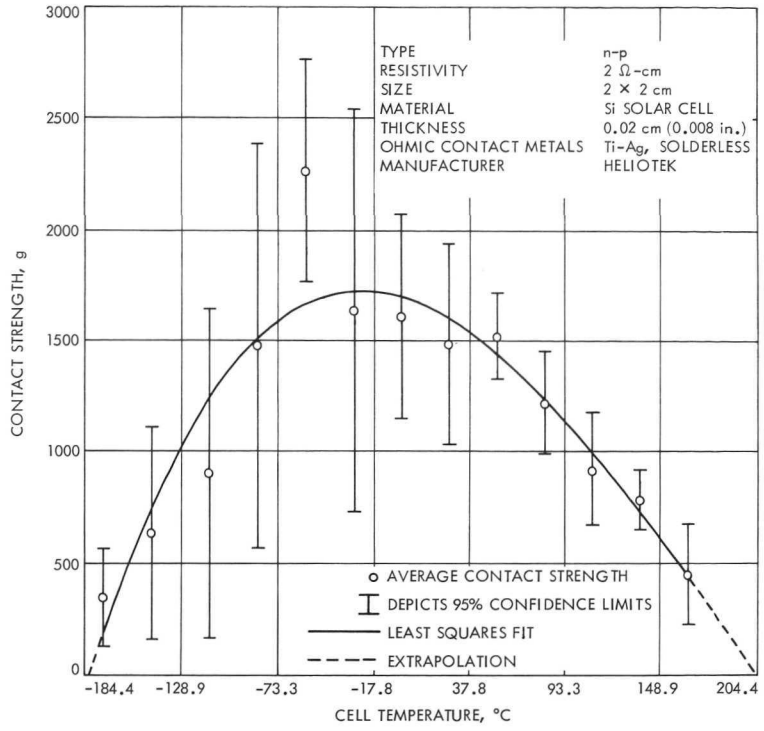

Fig. 19. *n*-contact strength, titanium–silver contacts on 0.2-mm-thick *n–p* cells, as a function of temperature

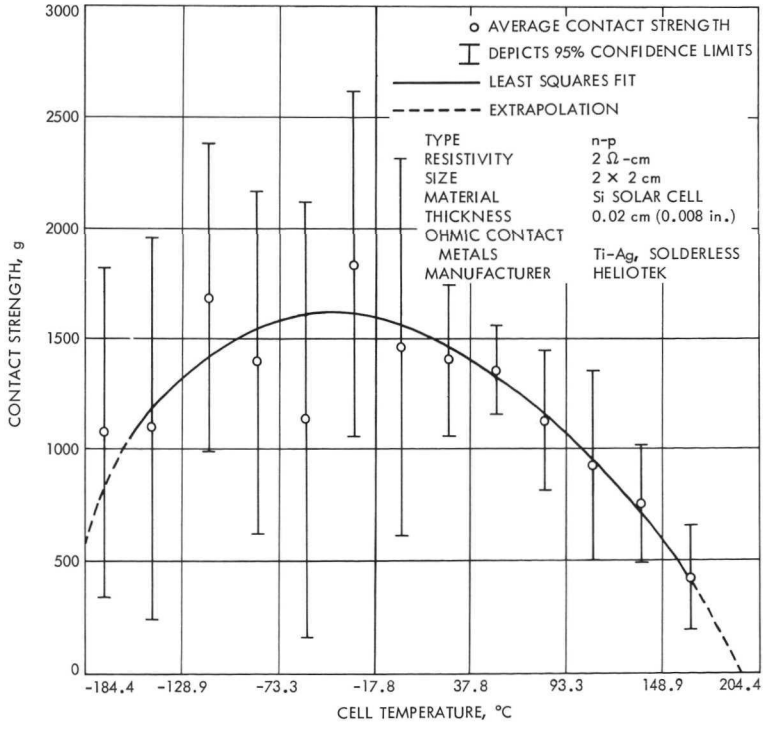

Fig. 20. *p*-contact strength, titanium–silver contacts on 0.2-mm-thick *n–p* cells, as a function of temperature

of silicone adhesive RTV-41 in conjunction with primer SS 4044 prior to the contact strength evaluations. Even with this precaution, a significant number of cells were broken during the pull tests. There did not, however, appear to be a discernible dependence of the number of broken cells on the pull test-temperature, as might be expected if thermal coefficient mismatches were responsible for the cell breakage. Thermal coefficient mismatches should result in significantly greater cell breakage at the extreme temperatures (largest ΔT).

The typical failure mechanism of the *n* or diffused-layer contact at temperatures between −173 and −112°C is shown in Fig. 21. It can be seen that massive silicon fracture has occurred, although the sharply defined structure seen in Fig. 7 (typical of the solder-coated titanium–silver contacts) is not observed. The pattern of the silicon removed, as shown in Fig. 21, does have a certain amount of regularity and follows the overall contours of the pull test tab. This is to be contrasted with the failure mechanism shown in Fig. 22, which depicts a typical failure between temperatures of −29 and −84°C, the region of maximum pull strength, and which shows a highly irregular pattern of silicon removal not conforming to the overall dimension of the pull test tab. This indicates excellent adherence of the tab and contact to the silicon, and also high silicon strength, since, in this temperature region, failure did not occur until an applied load of 1700 g was imposed. Thus, in Fig. 22, massive silicon removal indicates a good contact, whereas, in Fig. 21, the massive silicon removal indicates highly stressed silicon. As discussed previously, massive silicon removal must be interpreted judiciously with respect to the efficacy of the contact system in achieving high reliability.

A typical contact failure mode over the temperature range between −1 and +82°C is shown for the *n* contact in Fig. 23. This figure shows separation at the contact itself and cell breakage, but not the massive silicon removal observed at lower pull-test temperatures, as shown in Figs. 19 and 20.

A typical failure mode at temperatures between 110 and 165°C is shown for the *n* contact in Fig. 24, where there is a very clean and complete removal of the contact test tab from the cell, because of the increased plasticity and consequently lower adherence of the solder preform.

Similar results are shown for the *p* or base region contact in Figs. 25–28. The typical contact failure mode at low temperatures is shown in Fig. 25, which exhibits the massive silicon removal due to the silicon stress similar to that observed on the *n* contact over the same temperature range. Separation of the contact metals from the silicon surface and silicon removal are shown in Fig. 26 for pull tests performed at temperatures between −29 and −84°C. The prevalent failure mode at temperatures between −1 and +82°C is shown in Fig. 27, which indicates removal of the contact metals from the silicon surface and massive silicon removal that does not follow the geometry of the test tab. This type of silicon removal does not indicate silicon stress but relatively good contact adherence. The contact failure mode at high temperatures is shown in Fig. 28, which, as in the case of the *n* contact at these temperatures, indicates clean removal of the test tab because of the increasing plasticity and decreasing strength of the solder used to connect the test tab.

Table 5. Test conditions, solder-coated electroless-nickel-plated contacts on *p–n* cells[a]

Number of cells tested[b]	Test temperature	
	°C	°F
5	−173.3	−280
5	−145.6	−230
5	−112.2	−170
5	−84.4	−120
5	−56.7	−70
5	−28.9	−20
5	−1.1	30
5	26.7	80
5	54.4	130
5	82.2	180
5	110.0	230
5	137.8	280
5	165.5	330
0	190.5	375
0	204.4	400
0	218.0	425

[a]Base resistivity = 2 Ω-cm
Nominal dimensions
Size = 1 × 2 cm
Thickness = 0.046 cm (18 mils)
Vendor—Heliotek.
Flight history—*Mariner* 1962, *Mariner* 1971, and *Surveyor*.
[b]Total number of contacts evaluated ($p + n$) = 130.

D. Solder-Coated Electroless-Nickel-Plated Contacts on *p–n* Cells

The cell description and the number of cells tested at each temperature are shown in Table 5. A total of 65 cells was evaluated, corresponding to testing of 130 contacts. Cells of this type have been used in the *Ranger*, *Mariner*, and *Surveyor* flight programs. The contact strength of the *p* or diffused-sheet contact as a function of cell temperature is shown in Fig. 29. This figure, which shows the

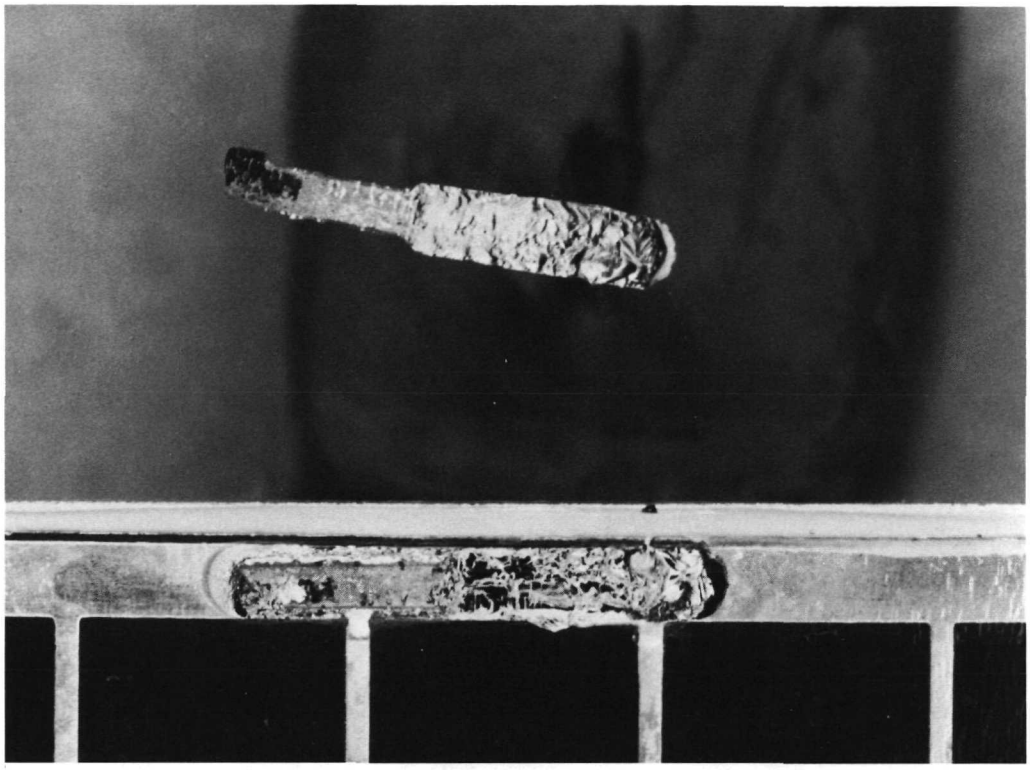

Fig. 21. Typical failure mode of *n* contact, titanium–silver contacts on 0.2-mm-thick *n–p* cells, over a pull-test temperature range of −112 to −173°C

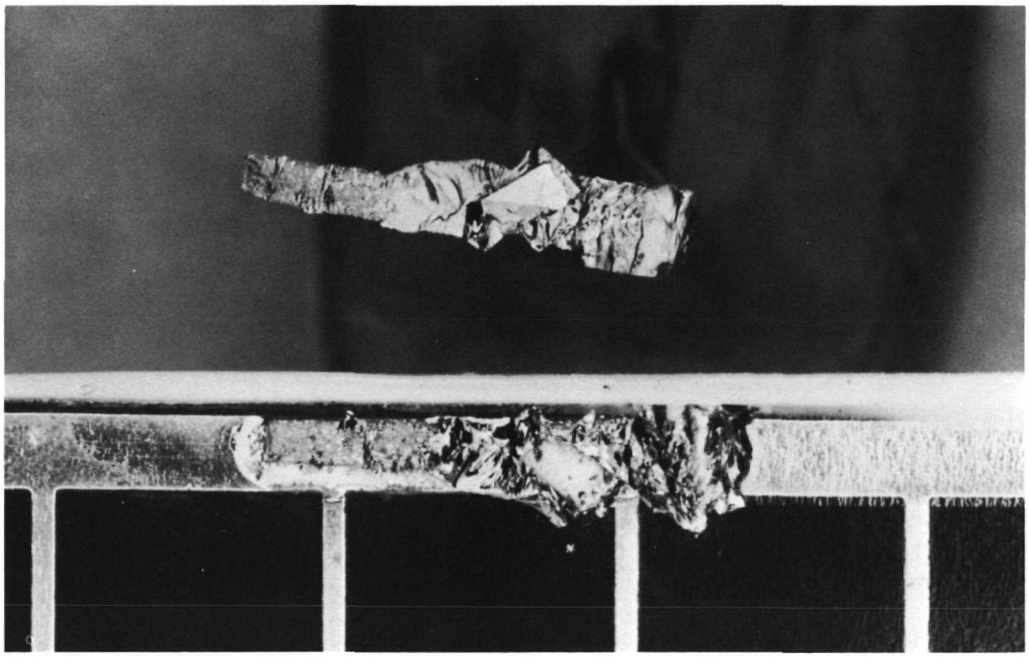

Fig. 22. Typical failure mode of *n* contact, titanium–silver contacts on 0.2-mm-thick *n–p* cells, over a pull-test temperature range of −29 to −84°C

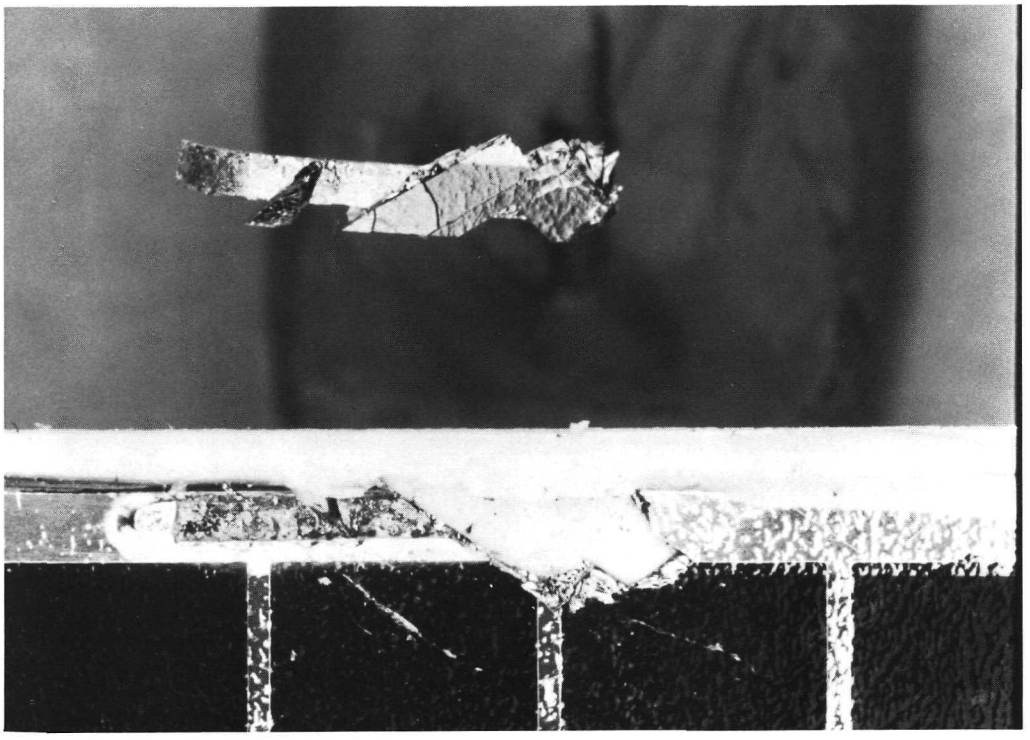

Fig. 23. Typical failure mode of *n* contact, titanium–silver contacts on 0.2-mm-thick *n–p* cells, over a pull-test temperature range of −1 to +82°C

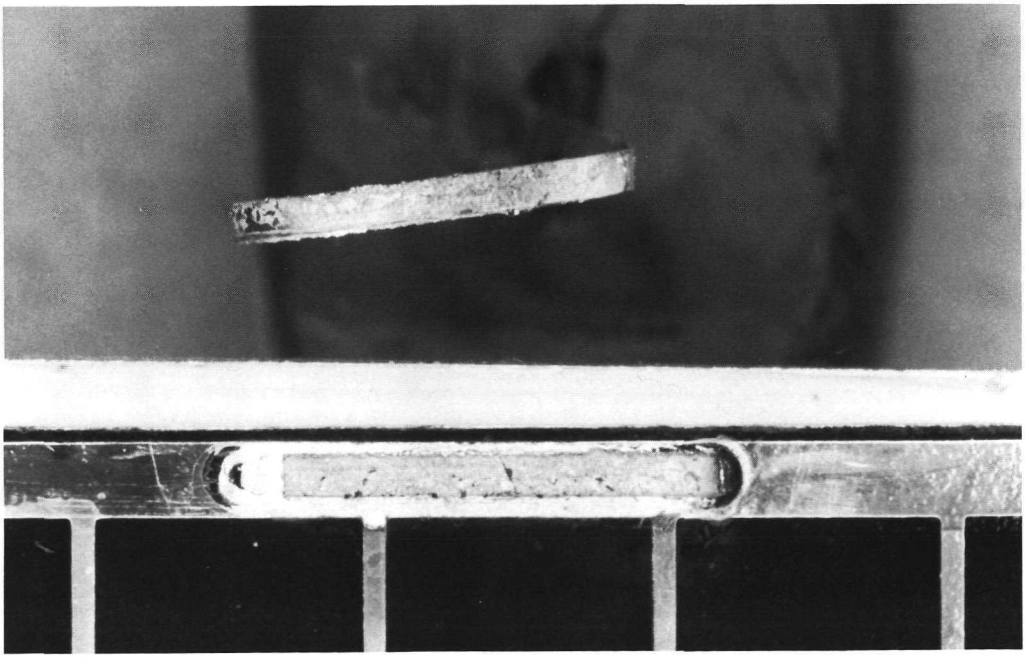

Fig. 24. Typical failure mode of *n* contact, titanium–silver contacts on 0.2-mm-thick *n–p* cells, over a pull-test temperature range of +110 to +165°C

Fig. 25. Typical failure mode of *p* contact, titanium–silver contacts on 0.2-mm-thick *n–p* cells, over a pull-test temperature range of −112 to −173°C

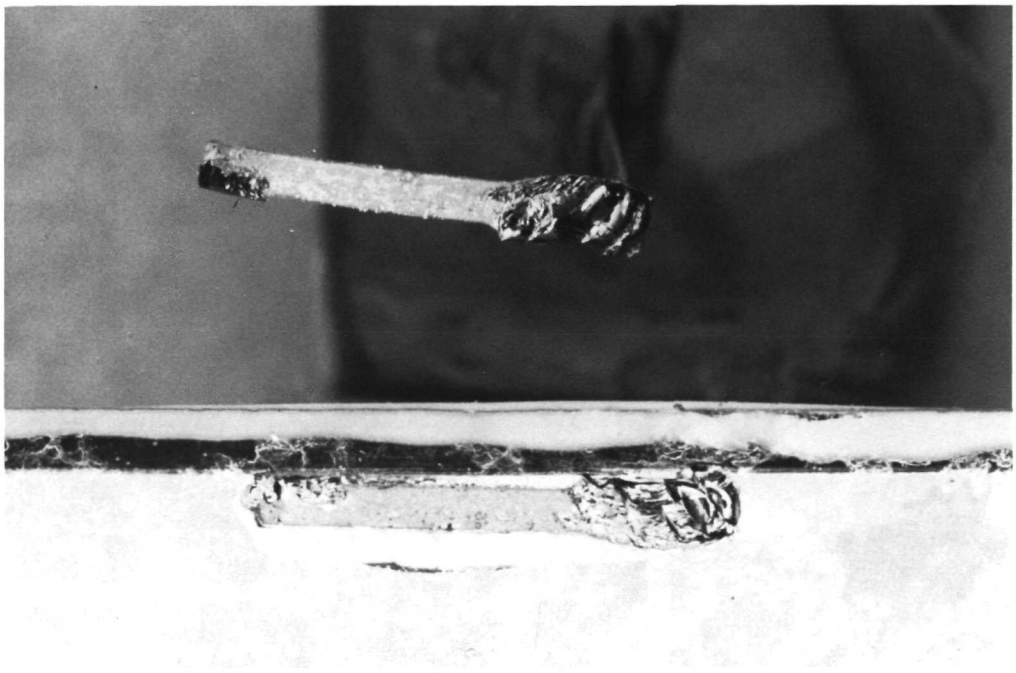

Fig. 26. Typical failure mode of *p* contact, titanium–silver contacts on 0.2-mm-thick *n–p* cells, over a pull-test temperature range of −29 to −84°C

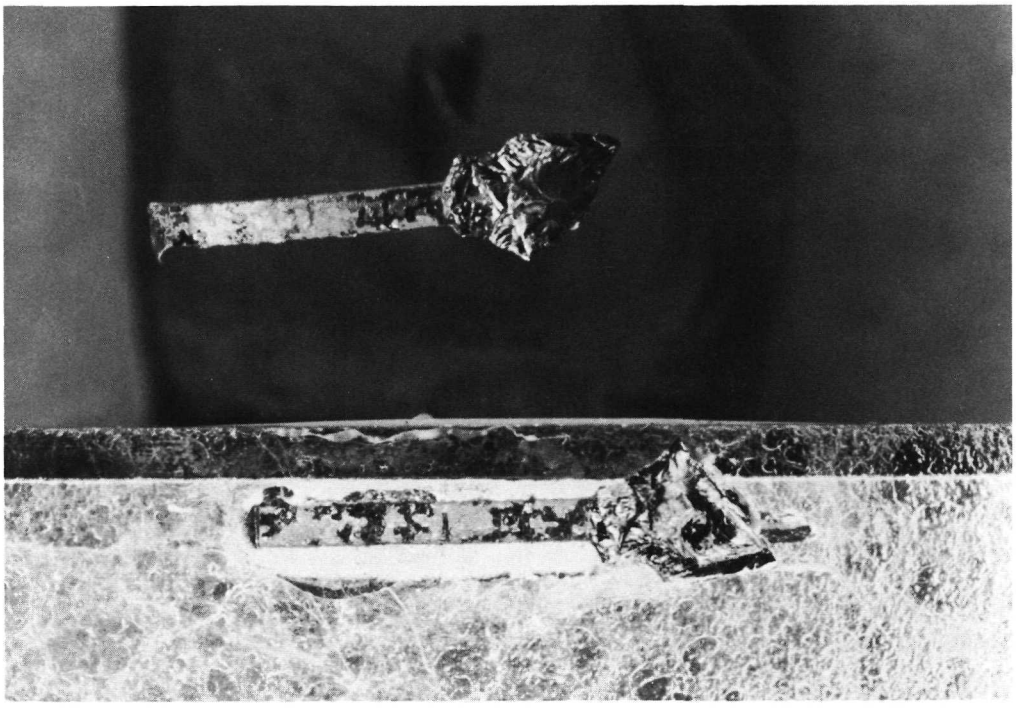

Fig. 27. Typical failure mode of *p* contact, titanium–silver contacts on 0.2-mm-thick *n–p* cells, over a pull-test temperature range of −1 to +82°C

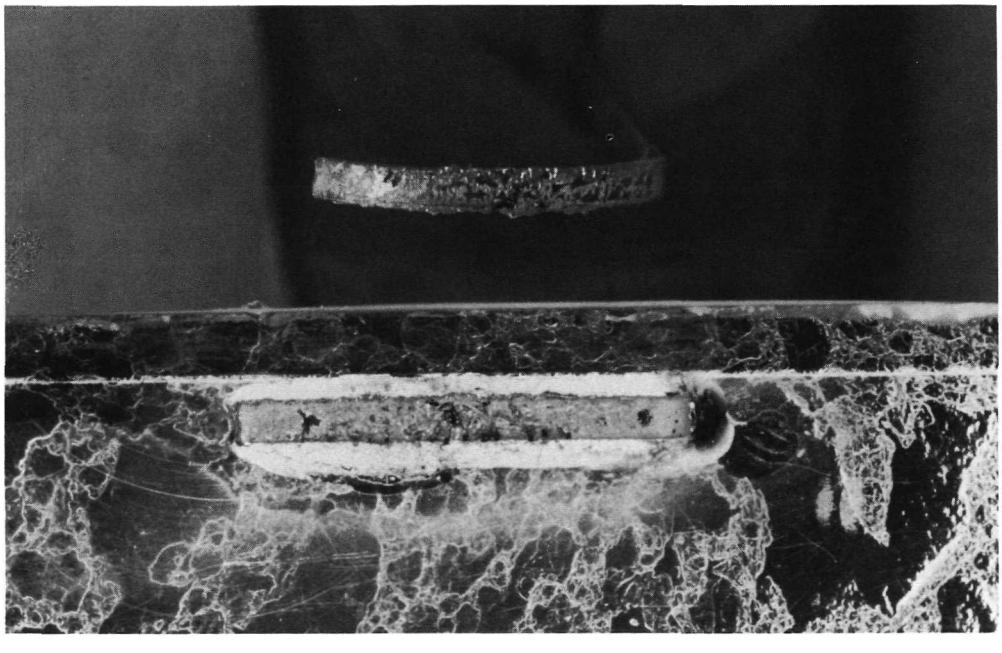

Fig. 28. Typical failure mode of *p* contact, titanium–silver contacts on 0.2-mm-thick *n–p* cells, over a pull-test temperature range of +110 to +165°C

average contact strength at each of the test temperatures, the 95% confidence limits, and a least squares fit to the data, should be compared with Figs. 5, 15, 17, and 19, which show the diffused-sheet contact strength of the solder-coated titanium–silver, palladium-containing titanium–silver, and titanium–silver contact systems, respectively. In Fig. 29, the maximum contact strength occurs at a higher temperature (approximately +27°C) than for the previous three contact systems. Also, the maximum contact strength of the solder-coated electroless nickel appears to be higher than those of the previous three contact systems, and this higher strength is maintained at the high and low temperature extremes investigated. Furthermore, the 95% confidence limits appear to be narrower over the temperature range of +27 to +82°C than the other contact systems.

The contact strength of the *n* or base region contact is shown as a function of cell temperature in Fig. 30. There are significant differences between the *n* contact pull-strength test results of Fig. 30 and the *p* contact strength test results of Fig. 29. First, the maximum contact strength appears to be achieved at a lower temperature (approximately −57°C). Second, the maximum contact strength and the contact strength at the high and low temperature extremes are considerably below those observed for the *p* contacts. Third, a very large spread in results is indicated by the 95% confidence limits over the temperature range of −146 to +110°C. These drastic differences between the diffused-sheet and base-region contact strength characteristics, which were not observed in the previous three evaporated contact systems, are probably due to the fact that the electroless nickel deposition depends upon a displacement plating reaction that is strongly affected by the surface conditions and the amount of dopant near the surface upon which the plating is to be deposited. Apparently the heavily boron-doped diffused-sheet surface is more amenable to formation of uniformly high-strength contacts deposited by this process than is the relatively lightly phosphorus-doped base-region surface.

A typical failure mode observed over the temperature range between −112 and −173°C for the diffused-sheet *p* contact is shown in Fig. 31. Massive silicon fracture can be observed on the separated contact pull-test tab and on the remaining cell surface. The pattern of the silicon removal exhibits the regularity indicative of fracture along specific crystalline planes.

The failure mechanism prevalent for the *p* or diffused-sheet contact over the temperature range of −29 to −84°C is shown in Fig. 32. While the cell has actually broken, probably due to a strain or microcrack in the silicon blank, this was not a prevalent failure mode. The object of note in this figure, representative of the failure mode observed in this temperature range, is the removal of the contact plating from the silicon surface, which is dramatically shown in this figure.

Over the temperature range of −1 to +82°C, the prevalent failure mode was the breakage of the cell as shown in Fig. 33, along with removal of the plating from the silicon surface. It has recently been found in the JPL lithium-doped solar cell development program, which utilizes the *p* diffused into *n*-base structure, that the normal boron trichloride diffusion techniques used to fabricate these cells results in very high stresses and very high dislocation densities in the silicon blank. This is probably the cause of the very high number of broken cells observed in the pull strength tests of the *p–n* cells investigated here.

The failure mechanism associated with the pull-strength tests of the diffused-layer contact over the temperature range of 110 to 165°C is shown in Fig. 34, which shows that the dominant failure mechanism was a reduction in the solder strength at these temperatures, where the solder tends to become plastic. There was also some removal of the plating from the silicon surface.

Similar results are shown for the *n* or base-region contact pull tests in Figs. 35–38. The massive silicon removal usually observed at low temperatures can be seen in Fig. 35, in which the silicon on the failed test tab and the remaining surface exhibits a regularity of pattern indicative of stress along crystallographic planes. Over the temperature range of −29 to −84°C, the failure mechanism is composed of silicon fracture and removal of the plating from the silicon surface, as shown in Fig. 36. Over the temperature range of −1 to +82°C, the predominant failure mechanism was removal of the plating from the silicon surface, as shown in Fig. 37. Over the temperature range of 110 to 138°C, the primary failure mechanism was again removal of the plating from the silicon surface, while at the highest temperature of +165°C, the failure mechanism was composed of both plating removal and loss of adherence of the solder. Typical plating removal at these temperatures is shown in Fig. 38.

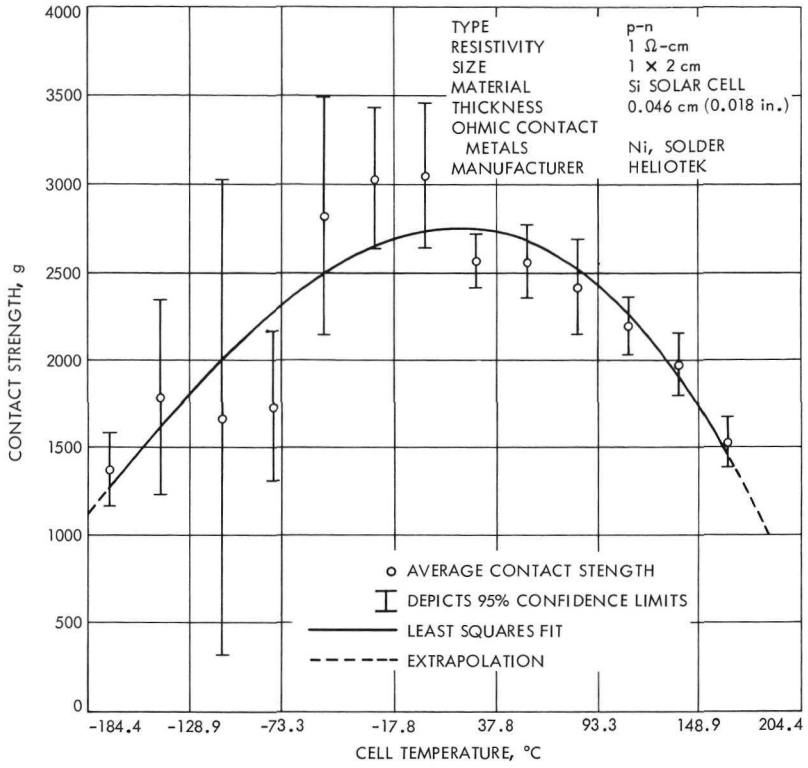

Fig. 29. *p*-contact strength, solder-coated electroless-nickel-plated contacts on *p–n* cells, as a function of temperature

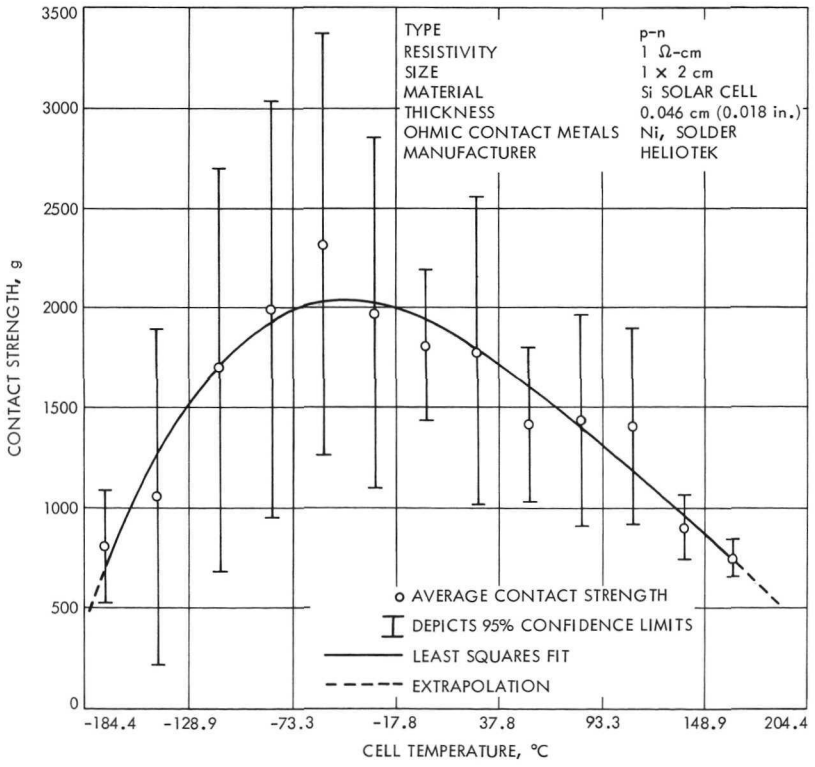

Fig. 30. *n*-contact strength, solder-coated electroless-nickel-plated contacts on *p–n* cells, as a function of temperature

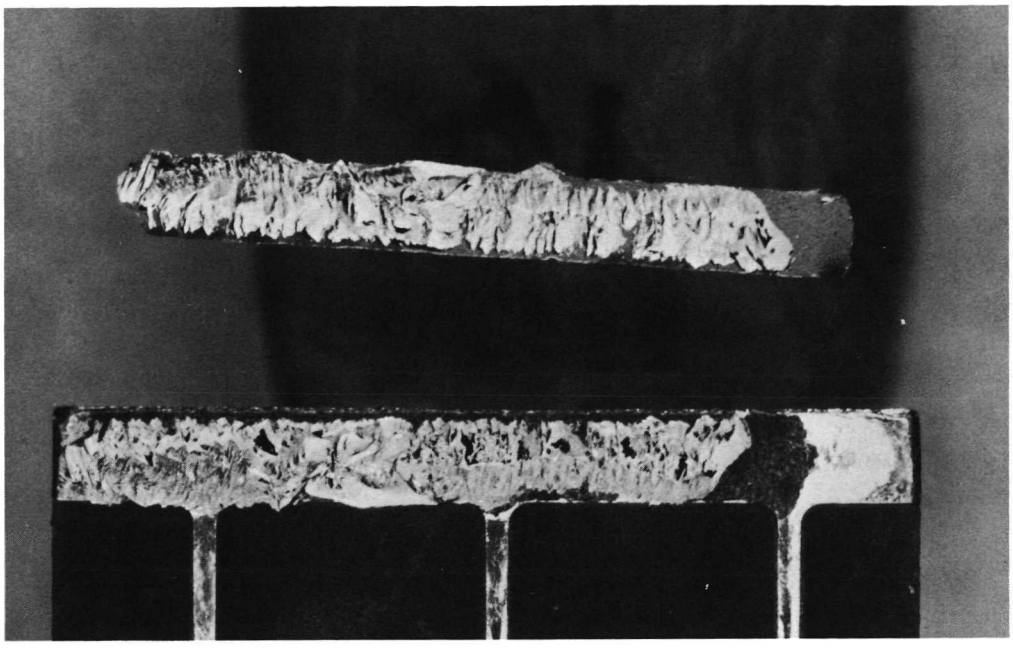

Fig. 31. Typical failure mode of *p* contact, solder-coated electroless-nickel-plated contacts on *p–n* cells, over a pull-test temperature range of −112 to −173°C

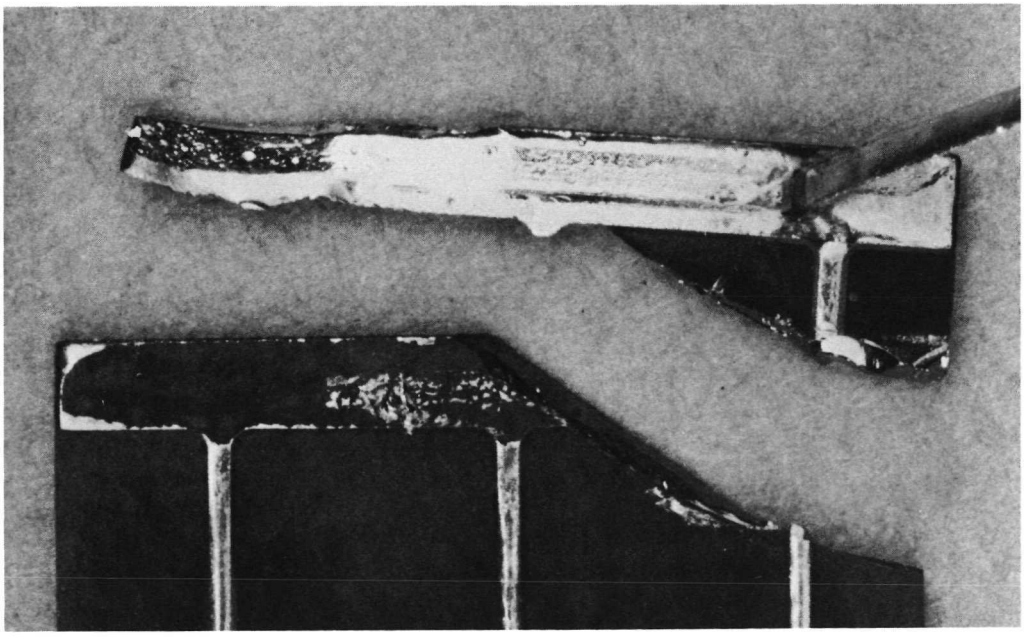

Fig. 32. Typical failure mode of *p* contact, solder-coated electroless-nickel-plated contacts on *p–n* cells, over a pull-test temperature range of −29 to −84°C

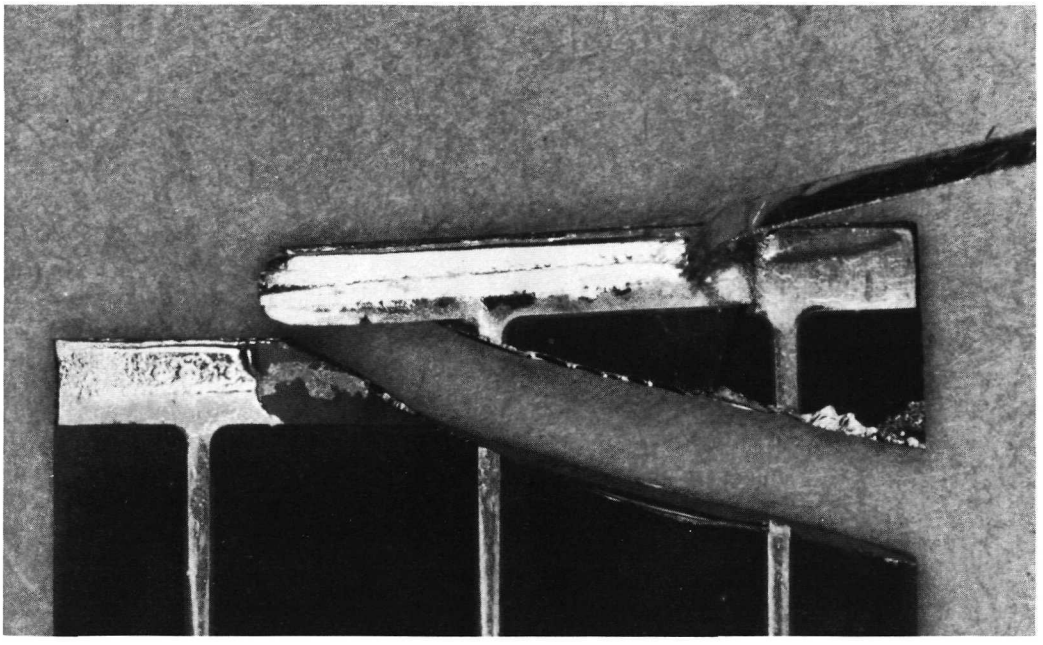

Fig. 33. Typical failure mode of *p* contact, solder-coated electroless-nickel-plated contacts on *p–n* cells, over a pull-test temperature range of −1 to +82°C

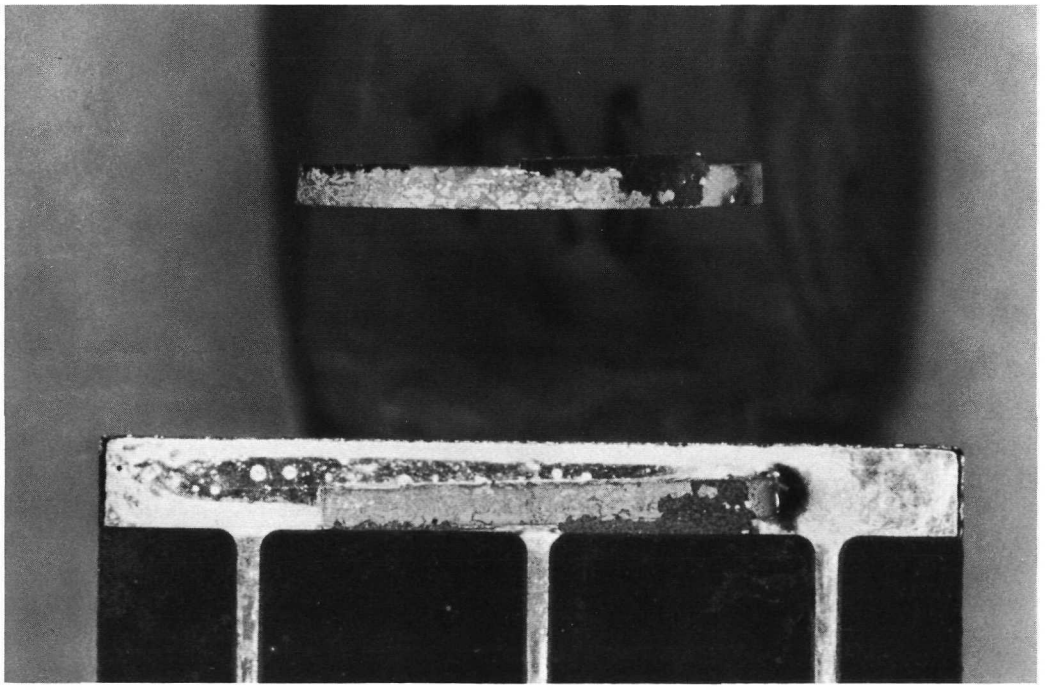

Fig. 34. Typical failure mode of *p* contact, solder-coated electroless-nickel-plated contacts on *p–n* cells, over a pull-test temperature range of +110 to +165°C

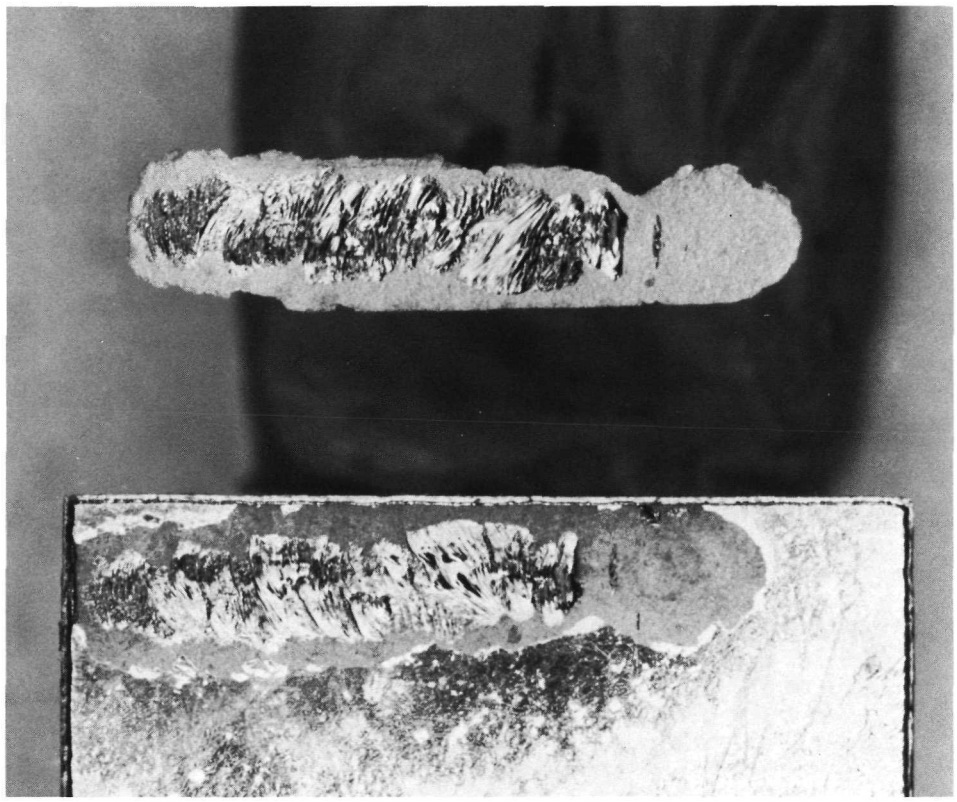

Fig. 35. Typical failure mode of *n* contact, solder-coated electroless-nickel-plated contacts on *p–n* cells, over a pull-test temperature range of −112 to −173°C

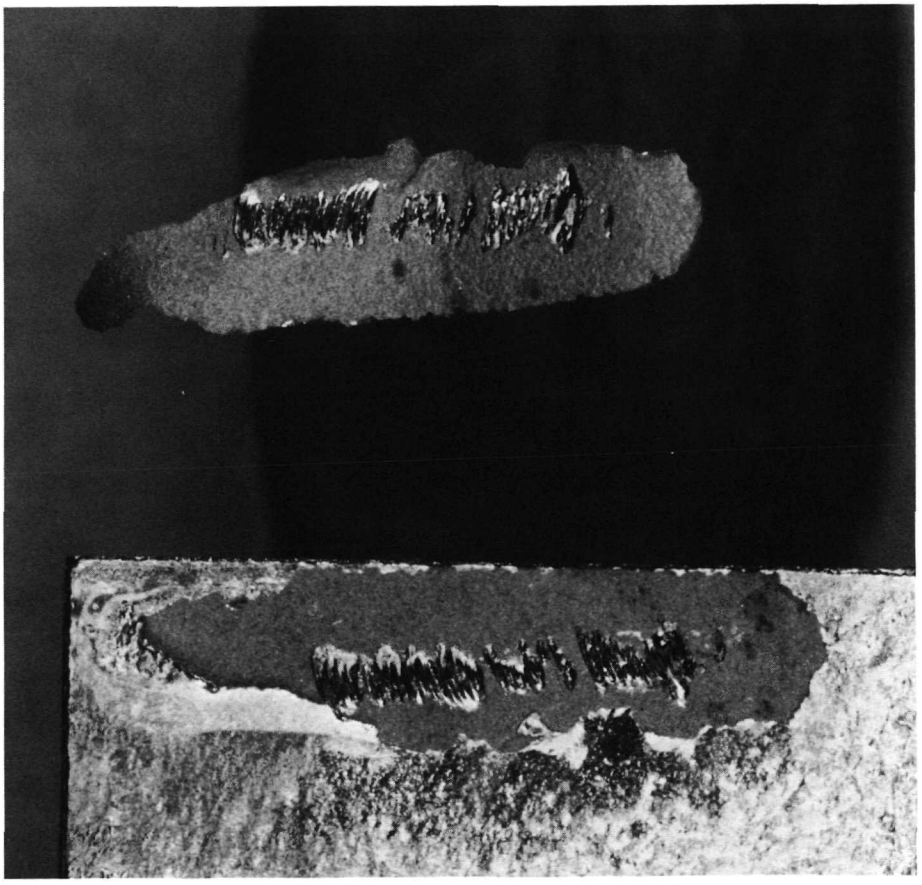

Fig. 36. Typical failure mode of *n* contact, solder-coated electroless-nickel-plated contacts on *p*–*n* cells, over a pull-test temperature range of −29 to −84°C

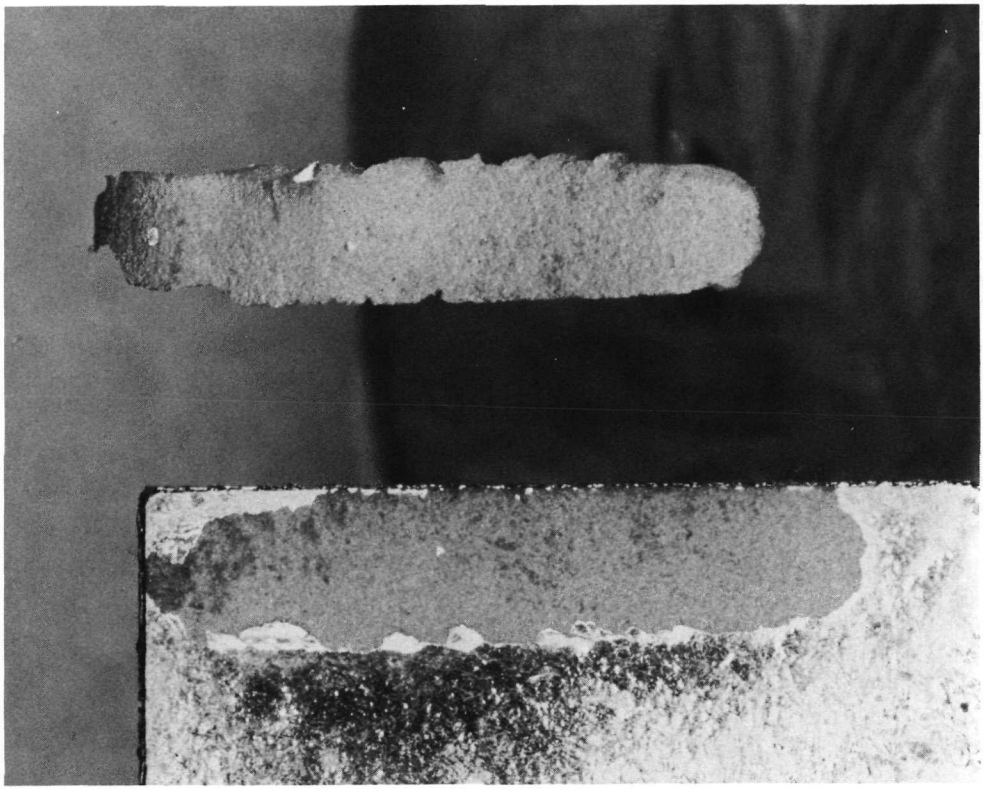

Fig. 37. Typical failure mode of *n* contact, solder-coated electroless-nickel-plated contacts on *p–n* cells, over a pull-test temperature range of −1 to +82°C

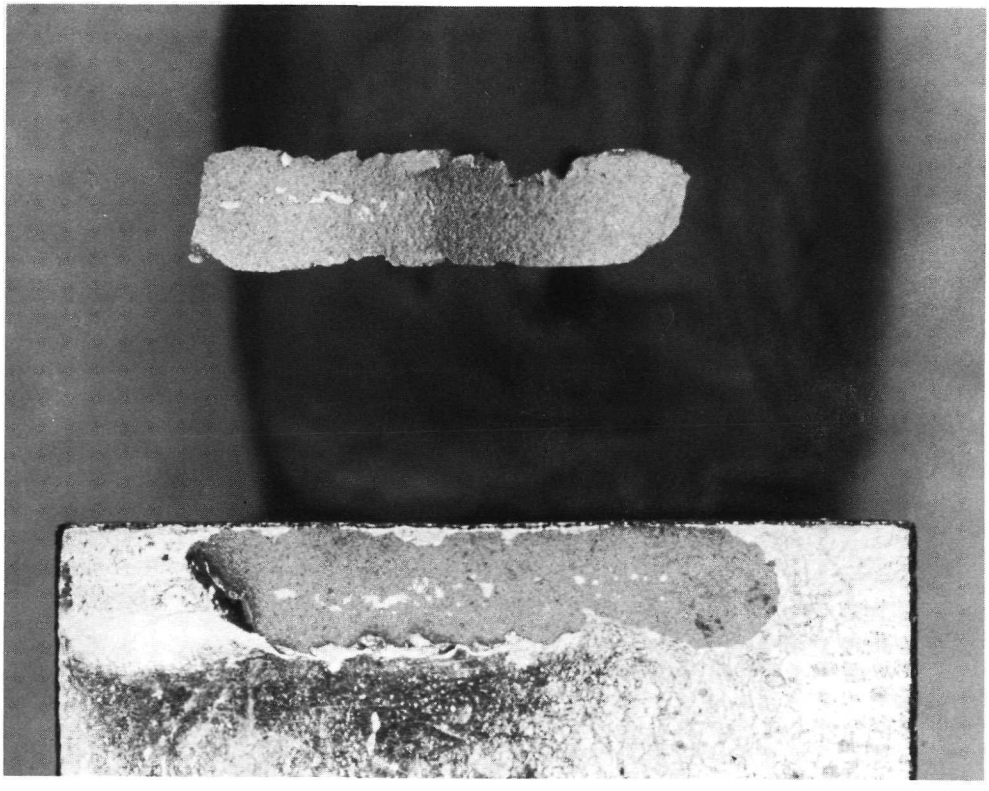

Fig. 38. Typical failure mode of *n* contact, solder-coated electroless-nickel-plated contacts on *p–n* cells, over a pull-test temperature range of +110 to +165°C

IV. Discussion and Conclusions

It has been conclusively shown that the mechanical strengths of the contact systems investigated here are a strong function of the temperature at which the contact pull tests are performed. In general, maximum pull strengths were achieved below 0°C.

At low temperatures the predominant failure mechanism is silicon fracture, as characterized by massive silicon removal with regular patterns observed in the silicon, corresponding to fracture along crystallographic planes. In this case, removal of silicon does *not* indicate a desirable contact system. Cells utilizing solder coating appear to be particularly vulnerable to this failure mechanism.

At intermediate temperatures, a combination of failure mechanisms is observed, consisting of silicon fracture, nonstructured silicon removal, delamination of the contact metal or metals from the silicon surface, delamination within the contact metals (to such an extent that contact material remains both on the cell surface and on the pull test tab), and removal of solder.

At the higher temperatures, the predominant failure mechanism is poor solder adherence due to the increased plasticity of the solder and loss of solder strength.

For the electroless nickel-plated contacts on p–n cells, the excessive cell breakage that was also noted was probably due to large stresses occurring in the cell blank as a result of the boron trichloride junction diffusion.

At the low and high temperature extremes, the spread in pull-test results was, in general, smaller than at the intermediate temperatures. This difference occurs because only one failure mechanism predominates at the low and at the high temperatures, namely, silicon fracture and loss of solder adherence, respectively, whereas many failure modes are operating and competing at the intermediate temperatures.

In agreement with the results of previous studies of effects of temperature and temperature–humidity storage environments on the strength of various contact systems (Refs. 1 and 2), the palladium-containing titanium–silver contacts exhibited lower absolute contact pull strengths than the other contact systems investigated here. This should not be interpreted as a condemnation of the palladium-containing titanium–silver contact system. The test data does indicate a wide variability in pull-contact strength, suggesting that major factors contributing to these results are the manufacturing process controls employed in making the cells. In fact, a general conclusion is drawn that process controls for all contact systems investigated could be significantly improved, since cells having ostensibly the same contact system exhibited in some cases very high contact strengths and in some cases very low contact strengths under the same test conditions.

For solder-coated cells, it is extremely important to control and minimize the solder thicknesses, particularly if the cells are to be exposed to low temperatures.

For solder- and non-solder-coated cells, particular attention must be paid to controlling the evaporation or plating parameters and the surface condition of the cell prior to evaporation or plating. One must take great pains to minimize surface contaminants by means of cleaning, etching, etc., and to ensure that the cells are not allowed to become recontaminated after the cleaning operations.

At the highest temperatures, where the failure mechanism appeared to be exclusively that of loss of solder tensile strength, performance could be improved only by utilizing a higher temperature melt solder (which may adversely affect the lower temperature characteristics) or by using solderless interconnection techniques such as welding or bonding.

Since it was generally observed that the maximum contact strength occurs at a temperature well below 0°C and drops off quite markedly at the normal cell operating temperature of 50 to 60°C (air mass zero equilibrium temperature) it would be highly advantageous to determine the factors that cause the maximum to occur at the lower temperatures and to utilize this to shift the maximum to the higher temperatures representative of those at which the cells will spend the majority of their time.

Particular attention has been given to the materials, processes, and techniques involved in performing pull-strength tests. This careful procedure has been found to greatly increase the reproducibility of the test results and is described in detail in this report. Some of the major parameters that must be controlled are the area on the cell contacts to which the contact test tabs are attached, the geometry of the test tab, the fabrication of the test tab from material such as Kovar (having a thermal coefficient of expansion approximating that of silicon), the minimization of variations in soldering technique (eliminating the effects of operator dependency), the proper composition, placement, and geometry of solder preforms if they are used (to prevent such detrimental effects

as silver scavenging in titanium–silver contacts), the careful inspection of the soldered pull-test tab and rejection of those that are questionable, and the careful control of the imposed pull rate.

Contact pull-strength tests represent one of the most important tools in evaluating the suitability of the cell for use in space missions. Such a test, however, is meaningful only to the degree that it does not itself introduce extraneous variables, so that the observed differences, if any, between cell contact systems can be ascribed to differences in either materials or techniques involved in cell manufacturing and not to differences due to variations in the testing techniques.

References

1. Yasui, R. K., and Berman, P. A., *Effects of High-Temperature, High-Humidity Environment on Silicon Solar Cell Contacts,* Technical Report 32-1520. Jet Propulsion Laboratory, Pasadena, Calif., Feb. 15, 1971.
2. Berman, P. A., and Yasui, R. K., *Effects of Storage Temperatures on Silicon Solar Cell Contacts,* Technical Report 32-1541. Jet Propulsion Laboratory, Pasadena, Calif., Oct. 15, 1971.
3. Moss, R., and Berman, P. A., *Effects of Environmental Exposures on Silicon Solar Cells,* Technical Report 32-1362. Jet Propulsion Laboratory, Pasadena, Calif., Jan. 15, 1970.
4. Salama, A. M., Rowe, W. M., and Yasui, R. K., *Stress Analysis and Design of Silicon Solar Cell Arrays and Related Material Properties,* Technical Report 32-1552. Jet Propulsion Laboratory, Pasadena, Calif., Mar. 1, 1972.
5. Butterworth, L. W., and Yasui, R. K., *Structural Analysis of Silicon Solar Arrays,* Technical Report 32-1528. Jet Propulsion Laboratory, Pasadena, Calif., May 15, 1971.

NASA — JPL — Coml., L.A., Calif.